The Pennsylvania State University
The Graduate School

UNDERSTANDING CURE INHIBITION IN CARBON FIBER REINFORCED VINYL ESTER RESIN COMPOSITES

A Thesis in
Materials Science and Engineering
by
Sean P. Tweed-Kent

© 2008 Sean P. Tweed-Kent

Submitted in Partial Fulfillment
of the Requirements
for the Degree of

Master of Science

December 2008

The thesis of Sean P. Tweed-Kent was reviewed and approved* by the following:

James Runt
Professor of Polymer Science
Thesis Co-Adviser

Thomas Juska
Assistant Professor of Materials Science and Engineering
Thesis Co-Adviser

Ronald Hedden
Assistant Professor of Materials Science and Engineering

Gary Messing
Head, Department of Materials Science and Engineering

*Signatures are on file in the Graduate School.

Abstract

The effect of neat and oxidized carbon fiber reinforcements on vinyl ester resin free radical polymerization was investigated. First, the free radical polymerization of neat vinyl ester resin, vinyl ester resin reinforced by neat carbon fibers, and vinyl ester resin reinforced by oxidized carbon fibers was analyzed with DSC. Neat carbon fibers, and to a greater extent oxidized carbon fibers, were observed to inhibit vinyl ester cure. Second, the surface chemistry of neat and oxidized carbon fibers was analyzed with XPS, NEXAFS, and ATR-FTIR. The surface characterization of neat carbon fibers identified carbon, oxygen, nitrogen, and several trace elements, including silicon, sodium, chlorine, sulfur, magnesium, and calcium. Neat carbon fiber spectra provided evidence for the presence of hydroxyls, ethers, carbonyls, oxidized nitrogen, nitrogen bound to carbonyls, quaternized nitrogen, and non-quaternized nitrogen. The most significant impact of oxidation on carbon fiber surface chemistry was the increase in features indicative of hydroxyls, carbonyls, and non-quaternized nitrogen. These functional groups are present on common inhibitors of free radical polymerization, such as phenols, quinones, and aromatic nitro-compounds, and are likely the cause of the vinyl ester resin cure inhibition observed with DSC.

Table of Contents

List of Figures

List of Tables

Acknowledgments

This work would not have been possible without the support and encouragement of my advisors, Jim Runt and Tom Juska. I thank Tom Juska for his valuable insight that greatly benefited this work. In Jim Runt, I could not have asked for a better advisor. His guidance and patience, especially through some early experimental struggles, were critical to the success of this project. I also thank Ron Hedden for serving on my committee and for taking time to discuss my research.

I wish to express my gratitude to the Penn State - Applied Research Laboratory Exploratory and Foundational Program for funding this project, and for their commitment to basic research and our national defense. Additionally, I appreciate Robert Schaut for sharing his knowledge of NEXAFS, Vince Bojan for his help in interpreting XPS, and Josh Stapleton for his support with ATR-FTIR.

I owe a special thanks to Robert Klein, an amazing friend with a bright future. I am indebted to him for collecting NEXAFS data, a pleasant surprise and a significant contribution to this work. I learned a great deal from him and enjoyed our many conversations.

I will always be grateful to John Creek for providing such a warm welcome to Happy Valley, for throwing great tailgates, and for turning me on to libertarian philosophy.

I wish to thank Greg Larsen for being a great flatmate, Greg Hogshead for our frequent coffee room encounters, and Rebeca Hernandez for introducing "Coffee Time".

I was extremely lucky to meet many amazing friends during my time at Penn State, including but not limited to: Justin Langston, Matthew Heidecker, Theresa Foley, Javier Sacristan, Wenjuan Liu, Kevin Masser, Noi Atorngitjawat, Suphannee Pongkitwitton, Daniel Fragiadakis, Perumal Ramasamy, Harshad Patil, Fidel Castro-Marcano, Alicia Castagna, Amanda McDermott, and Michelle Hill.

I thank my sisters, Shannon and Ailis, and my brothers, Michael, Christopher, and Daniel for all of their love and support.

Finally, I thank my wife and best friend, Marita, for her love and support. Without her companionship I would not be nearly as successful or happy. I left State College with many great memories, but the greatest was the birth of my daughter, Acadia, whose inquisitive and optimistic nature are a joy to behold.

Dedication

To my parents, who have made countless sacrifices on my behalf that I am only now beginning to appreciate.

Chapter 1

Introduction

1.1 Motivation

The development of materials enabling weight reduction and performance improvement remains a significant challenge for a broad spectrum of applications. Advanced composite materials are a potential solution for these challenges. Recently, carbon fiber composites have been selected by the U.S. Navy for use in advanced lightweight ship structures. Compared to traditional ship building materials, such as steel or aluminum, carbon fiber composites have superior specific strength, specific stiffness, corrosion resistance, and the potential for reduced maintenance costs. Additionally, carbon fiber composites offer improved stealth capability with lower magnetic, acoustic, hydrodynamic, radar, and thermal signatures.[5]

Thus far, structures composed of carbon fiber reinforced vinyl ester resins have failed more easily than expected under transverse loading. These problems are thought to arise from poor fiber-matrix adhesion, a relationship first proposed by Dr. Thomas Juska in 1993.[3,6,7,8,9,10] Research to improve adhesion by adjusting fiber surface properties has produced limited and unsatisfactory progress.[3,9,11,12,13,14] Although these efforts have produced some generally helpful structure-property relationships, a clear understanding of the underlying mechanisms remains elusive.

Meanwhile, it was observed at the Penn State Applied Research Laboratory that carbon fibers oxidized in air at elevated temperatures produced composite structures with vinyl

ester resins that exhibited macroscopic qualities indicative of cure inhibition.[15] This thesis aims to understand the structure-property relationships behind these observations as part of the broader effort to realize the significant application potential of carbon fiber reinforced polymer composites.

1.2 Vinyl ester resins

Today, thermosetting polymer systems represent around two-thirds of all matrix resins used in fiber reinforced polymer composites.[16] Unsaturated polyester resins are the most common thermosetting matrix resin, but other important thermosetting resins include epoxy, polyurethane, phenolic, and the system of interest in this study, vinyl ester, sometimes referred to as epoxy vinyl ester.[17]

Vinyl ester resins (VERs) were developed as an alternative to epoxies and unsaturated polyesters. The general vinyl ester structure is presented in Figure 1.1. Although epoxies offer superior mechanical properties and low shrinkage, they are more expensive than vinyl esters and their higher viscosity makes processing more difficult. Unsaturated polyester resins are easily processed and inexpensive, but poor mechanical strength limits their application. Overall, vinyl esters have an attractive combination of good mechanical strength, excellent corrosion resistance, low cost, high Tg, and low viscosity, making them well suited for a variety of applications. Unfortunately, interfacial adhesion in carbon fiber reinforced vinyl ester systems is reported to be half that of epoxy systems reinforced by the same carbon fibers.[8]

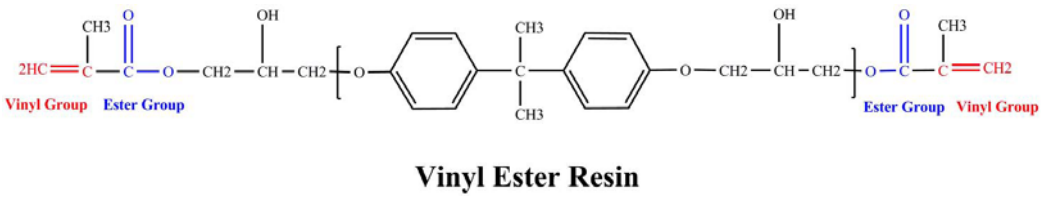

Figure 1.1. General structure of vinyl ester resin monomer.

Synthesis of vinyl ester resins are conducted via an addition reaction between a carboxylic acid and an epoxy resin. Vinyl ester monomers have a backbone structure similar to epoxies and terminal unsaturated vinyl groups.[18] After synthesis, vinyl esters are typically mixed with up to 50% styrene, a reactive diluent, to facilitate processing. Copolymerization between vinyl esters and styrene, as shown in Figure 1.2 , proceeds via free radical polymerization, and can occur at room temperature.[19,20,21] However, a source of free radicals is needed to initiate the reaction. Catalytic initiation is the most common, but thermal initiation is also possible. Catalytic systems usually involve an organic peroxide initiator and a reducing agent, termed a promoter or accelerator, such as cobalt napthenate (CoNap), and dimethylaniline (DMA). In many applications, fire retardancy is an important property. To improve fire retardancy, brominated vinyl esters are often used to limit flame spread and heat release rate.[22]

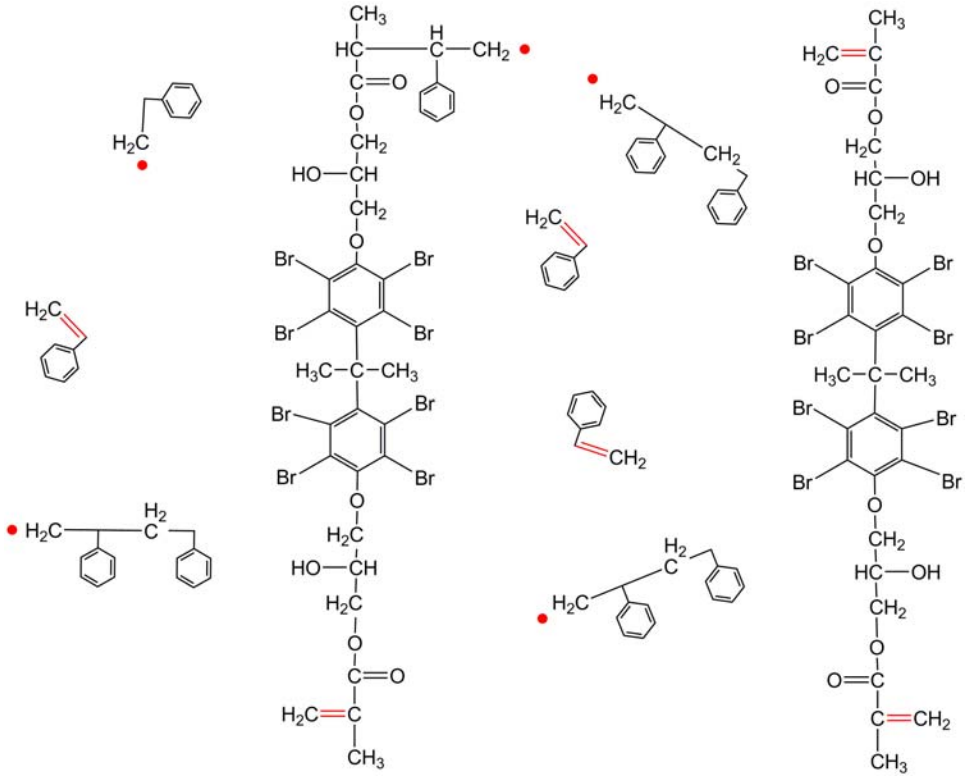

Figure 1.2. Schematic illustration of copolymerization between vinyl ester and styrene via free radical polymerization.

1.3 Historical development of carbon fiber reinforced vinyl ester composites

Fiber reinforced polymer composites are comprised of a polymer matrix and a reinforcing fiber. The matrix binds, protects, and transfers load between the reinforcing fibers. The origins of fiber reinforced polymer composites were established with the development of organic resins and synthetic fibers in the 1930s. By the 1950s, glass fiber reinforced polyester resins had become widely commercialized. About the same time, demand from the aerospace industry for high performance composites led to the development of carbon fibers.[16,23]

Carbon fibers are filaments, tows, yarns, or rovings consisting of at least 92% (mass fraction) carbon.[24] Their discovery dates back to Thomas Edison in 1880, who pyrolyzed cellulose based materials into carbon filaments for early light bulbs.[23] Modern carbon fibers were first developed in the 1950s at Union Carbide from rayon, a polymer fiber regenerated from cellulose. Polyacrylonitrile (PAN), another carbon fiber precursor, largely replaced rayon in the 1960s as a more economical alternative with simpler processing, better yield, and improved strength and stiffness. Carbon fibers synthesized from pitch, the first non-polymeric precursor, were developed in the 1970s. The main source of pitch is still the residue of petroleum refining or coal tar distillation.[16,25]

The substantial cost of carbon fibers was once the primary hurdle to more widespread application, but performance and fabrication costs are now of equal or greater importance. In the 1960s carbon fibers were $400-500 per pound, but currently standard and intermediate modulus fibers can be purchased for less than $20 per pound. This dramatic improvement in cost is the result of gains in production efficiency, and an oversupply resulting from reduced defense spending in the early 1990s. Lower prices have led to more commercial applications, ultimately reducing military usage of carbon fiber from 43% of the US market in 1989 to only 9% in 2003.[26] For example, 50% of the new Boeing 787 Dreamliner will be manufactured with advanced composites, specifically carbon/epoxy systems.[27]

Despite an acknowledged lack of carbon fiber industry statistics, a 2005 National Research Council report puts PAN-based carbon fiber worldwide market share at about 90%, with the rest primarily pitch-based.[26] In general, PAN produces fibers with higher specific strength, but lower specific modulus than those made from pitch.[16,26] The precursor choice depends on the strength and modulus required by a specific application.

Carbon fiber production from PAN involves the following general steps: spinning, stabilization, carbonization, and surface treatment.[16,26,28,29] First, the spun polymer fibers are stabilized via oxidation at 300°C. Although there is broad agreement that oxidation of spun polymer fibers increases thermal stability, the exact structure resulting from this step remains disputed.[29] Next, carbonization occurs at temperatures above 1000°C under an inert atmosphere, typically nitrogen. At these temperatures most non-carbon species are driven off, leaving fibers with at least 92% carbon and some residual nitrogen. Carbonization at temperatures above 2000°C is known as graphitization, and although fiber strength peaks at about 1500°C, modulus increases continuously up to around 3000°C.[16,29,30] However, the process of carbonization produces fibers with a relatively unreactive surface, prompting suppliers to provide a proprietary surface treatment. Surface treatments have been used effectively to promote fiber-matrix adhesion, an important factor in overall composite properties.

1.4 The interphase and fiber-matrix adhesion

In addition to the properties of the component materials, composite performance is critically dependent on efficient load transfer from the matrix to the reinforcing fibers. Efficient load transfer depends on good fiber-matrix adhesion in the interphase; a complex three dimensional region that is compositionally different than the bulk and not well understood.[9,12,26,31,32]. The term interface, as used in this thesis, refers to the quasi two dimensional region separating the fiber and matrix.

Fiber-matrix adhesion is most important to composites under compression, shear, and transverse loading. Both direct and indirect approaches of measuring adhesion are regularly used. Indirect testing of fiber-matrix adhesion is commonly performed using macromechanical techniques, such as short beam or four point shear. These methods determine composite properties that indirectly reflect fiber-matrix adhesion such as interlaminar shear strength (ILSS), in-plane shear strength, and transverse tensile strength. In these tests, shear failure involves a combination of matrix yielding and fiber-matrix debonding, complicating analysis.

Fiber-matrix adhesion can be directly measured using micromechanical techniques, such as microdebond or fiber pull-out. These methods determine interfacial shear strength (IFSS), a direct measure of fiber-matrix adhesion.[18,25,33,34,35] Although analytically more direct, micromechanical testing is experimentally more difficult, and since these tests are performed on single fibers, their results have limited application to actual composites.

Past and current efforts to improve fiber-matrix adhesion have primarily focused on controlling the interphase through carbon fiber surface treatment. Surface treatments are most often oxidative and include 'wet', 'dry', and electrochemical methods.[7,36] Although not always considered a treatment, carbon fibers are also commonly coated with a proprietary polymer film, a process known as sizing. Sizing protects the fibers from damage, facilitates handling, and has been shown to improve fiber-matrix adhesion.[3,37] Due to the proprietary nature of sizing and for the sake of simplification, unsized fibers were used in this study.

Although surface treatments have produced moderate gains in fiber-matrix adhesion, the impact of carbon fiber surface structure on the interphase and fiber-matrix adhesion is still not well understood. In general, fiber-matrix adhesion is controlled by chemical and mechanical interaction between the matrix resin and reinforcing fiber, illustrated in Figure 1.3. Some of the suggested mechanisms contributing to adhesion include chemical reactions between the fiber surface and matrix resin, van der Waals forces, electrostatic attractions, acid-base interactions, and mechanical interlocking, caused by diffusion of resin

into pores in the fiber surface.[9,12] Both increased surface roughness and oxidation have been shown to improve adhesion in thermosetting composite systems.[14] Each mechanism of adhesion is controlled by the carbon fiber surface chemistry and surface morphology, but a complete understanding of the relationship is not well understood.

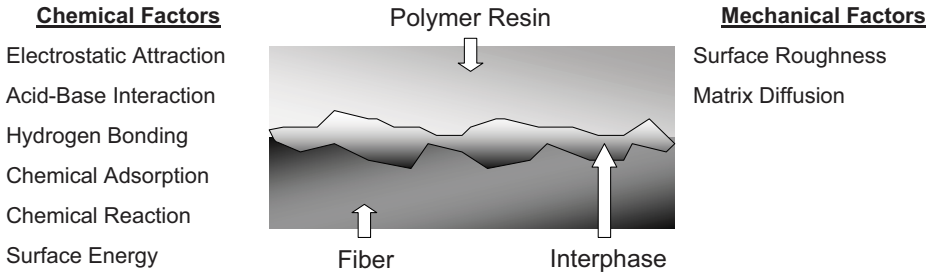

Figure 1.3. The chemical and physical mechanisms controlling fiber-matrix adhesion in the interphase.

After carbonization, the carbon fiber surface structure is occupied by planes of carbon molecules with atoms bound to each other by strong orbitals of sigma and pi electrons. The saturation of carbon atom valances inside these molecular planes decreases surface energy and reduces atomic activity.[38] As previously mentioned, surface treatments are an effective way to improve carbon fiber surface properties. One goal of such surface treatments is to functionalize the fiber surface. Functionalization increases surface reactivity, and facilitates chemical bonding with the matrix. Functionalization also increases the fiber surface energy, specifically the polar component, improving wettability, an important contributor to good adhesion. In addition to chemical bonding and wettability, surface functional groups can also facilitate adhesion through increased acid-base interactions and hydrogen bonding.

Surface morphology is also an important factor controlling adhesion. An increase in surface roughness facilitates surface functionalization by increasing surface area, and as a result, surface free energy. Increased surface roughness also improves mechanical interlocking by increasing the area of physical interaction between the fiber and matrix resin. Finally, the

removal of any weak boundary layer has been shown to significantly improve fiber-matrix adhesion by providing a stable substrate for the matrix resin to adhere to. Clearly, a good understanding of the carbon fiber surface and the role of specific properties on adhesion is critical to controlling overall composite properties.

1.5 Carbon fiber surface characterization

Many research groups have attempted to study the relationship between carbon fiber surface properties, fiber-matrix adhesion, and overall composite performance. An excellent review article by Sherwood describes the most common surface characterization techniques used to characterize the carbon fiber surface.[7] The most commonly applied technique is X-ray photoelectron spectroscopy (XPS). XPS is capable of identifying both elemental and functional changes in surface chemistry and it is truly surface sensitive, detecting only up to the first 100Å. Previous studies utilizing XPS to investigate surface treatment of carbon fibers generally report an increase in bound surface oxygen atoms. Several studies have also reported increases in bound surface nitrogen atoms. Low concentrations of sulphur, silicon, potassium, and sodium have also been reported, the source of which is almost universally attributed to fiber production and treatment processes.[8,13,39,40] One complication of XPS analysis is the need to deconvolute overlapping features to quantitatively identify specific functionalities, a process that introduces a moderate level of subjectivity.

Another method utilized in carbon fiber surface characterization is Fourier transform infrared spectroscopy (FTIR). Attenuated total reflectance (ATR) FTIR analysis is less surface sensitive compared with XPS, detecting species at depths on the order of 1 μm, and it is limited by strong carbon fiber absorption and scattering.[41] Despite these problems, several studies report ATR-FTIR spectra exhibiting an increase in carbonyl and hydroxyl functionality resulting from surface treatment.[7,42,43] To a lesser extent, quinone, ester and

phenol structures have also been suggested.[7,43,44]

To clarify some of the ambiguity surrounding XPS and FTIR analysis of carbon fibers, chemical reactions have been utilized to verify functional groups on the carbon fiber surface. These reactions include: the use of epichlorohydrin to confirm carboxylic acids; saponification with NaOH to test for carboxylic acids and esters; reaction with $LiAlH_4$ to identify carbonyls and carboxyls; the labeling of carboxylic acids with barium; and the reaction of diazomethane to detect hydroxyl functionality.[13,44,45]. Additionally, the selective and quantitative labeling of phenolic hydroxyl and (to a lesser extent) carboxyl groups has been done using vapor phase reaction with TFAA (trifluoroacetic anhydride).[46]

After characterizing fiber surface chemistry, some authors were able to identify important relationships between specific surface properties and fiber-matrix adhesion. In a study of carbon fiber reinforced epoxy, a direct relationship was reported between surface oxygen content, the polar component of surface free energy, and IFSS.[32,47,48] Another paper reported a correlation between increased carbon fiber surface acidity and an improvement in IFSS.[32,49] Two other investigations demonstrated that as the surface oxygen to carbon ratio increases, so do ILSS and IFSS.[50,51]

Several reports have also been published demonstrating an effect of reinforcements and fillers on matrix resin cure. One study on glass fiber reinforced vinyl ester reports a direct relationship between the polar component of fiber surface free energy and the activation energy of vinyl ester polymerization.[52] Other examples of reinforcements reported to affect resin cure include: the inhibition of unsaturated polyester resin cure due to the presence of untreated E-glass powder and glass beads[53,54]; the depression of both polyester and epoxy exothermic reactions due to fillers, most significantly with graphite[55]; and the correlation between cure exotherm and mechanical properties.[55]

One proposed explanation for the observed impact of reinforcements on matrix cure is chemisorption of matrix constituents by the fiber surface. Evidence has been presented

that cobalt adsorbs onto carbon fibers, an event likely to reduce polymerization rates near the fiber surface by decreasing the promoter concentration in solution.[3,45,52] Another possible explanation is a phenomenon known as the 'Trommsdorff' or 'gel' effect.[56] By limiting translational mobility of the reacting species, the presence of reinforcing fibers may aid radical trapping, which would decrease initiator efficiency and inhibit polymerization. However, limiting bimolecular termination could also increase free radical concentration, accelerating the reaction.[52]

It also appears that the observed improvements in fiber-matrix adhesion are not solely due to the effect of changes in surface chemistry. One report demonstrates that electrolytic surface treatment alters the mode of composite failure. While untreated fiber reinforced composites fail through the outer layer of the carbon fibers, surface treated fiber reinforced composites fail through the interphase. This observed change in failure mode suggests that the removal of a weak boundary explains, at least in part, the improved fiber-matrix adhesion resulting from carbon fiber surface treatment.[57] Another study shows that while the addition of surface oxygen content significantly improves IFSS, the subsequent removal of these additional oxygen groups (via high temperature vacuum treatment) does not eliminate all of the realized gains in IFSS.[32] These results confirm that, in addition to surface chemistry, surface roughness is an important factor controlling fiber-matrix adhesion.

1.6 Purpose of this study

Future growth of advanced composites in both commercial and military applications depends on continued reduction in fiber cost, and more importantly, further improvement in composite performance and property control. The previous description of the relationship between carbon fiber surface structure and fiber-matrix interaction makes it clear that control over the interphase region is critical. The fiber surface energy, functionality, wettability,

roughness, and preferential adsorption of reacting species all contribute to the final composite performance. A better understanding of the structure-property relationship remains an important challenge.

Unfortunately, carbon fibers are relatively difficult to study in a controlled manner. Most academic facilities cannot produce fibers, and thus they rely on industrial materials. A reliance on industry for materials introduces two major problems. First, using a supplier introduces an inherent lack of control. The fibers are produced, stored, and shipped under unknown conditions prior to receipt in the lab. Second, commercially produced materials are proprietary, making it difficult to obtain specific information about the materials or how they were manufactured. An important goal should be to improve collaboration and communication between industry and academia, which would address many of these issues and substantially improve research through better efficiency.

The goals of the research presented in this thesis are: (1) to identify what effect carbon fiber reinforcements have on vinyl ester polymerization and (2) to identify, through surface characterization, the changes in carbon fiber structure likely responsible for the observed effect. The effect of neat and oxidized carbon fiber reinforcements on vinyl ester polymerization is studied with differential scanning calorimetry (DSC). Changes in carbon fiber elemental and functional chemistry resulting from oxidation are investigated with XPS, near edge X-ray absorption fine structure (NEXAFS), and ATR-FTIR.

The author hopes that these results will further the scientific understanding of carbon fiber reinforced vinyl ester composites. With an improved understanding of structure property relationships, it may become possible to realize the full application potential of carbon fiber composite technology.

Chapter 2

Experimental

2.1 Materials

The fibers used in the present study were AS4 12K PAN based carbon fibers purchased from Hexcel. AS4 represents a Hexcel specific fiber type and the S in AS4 means that the fibers were subjected to Hexcel's proprietary surface treatment. The fibers arrived unsized with 12,000 filaments per tow, hence the 12K. To be clear, the as received fibers will be referred to as 'neat' fibers in this thesis. In order to investigate the impact of oxidative surface treatment on vinyl ester polymerization, the neat fibers were oxidized in air at 482°C for 6 hours. In DSC experiments, the composite system consisted of approximately 50% carbon fiber and 50% vinyl ester by weight. When not used for sample preparation all fibers were stored under nitrogen.

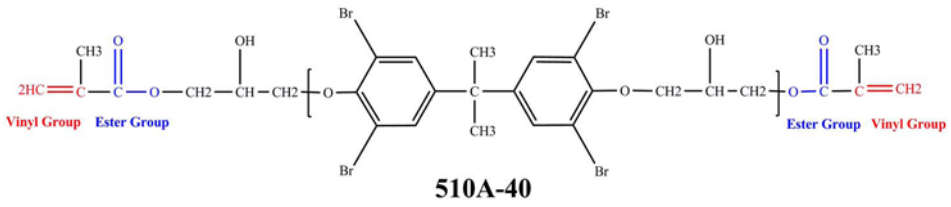

Figure 2.1. Chemical structure of 510A-40 brominated vinyl ester resin monomer.

The matrix resin utilized in the study was Derakane 510A-40 epoxy vinyl ester resin, a brominated bisphenol-A based vinyl ester resin diluted with 38% styrene. Figure 2.1 presents

the structure of 510A-40 vinyl ester. Although the free radical polymerization of vinyl ester was thermally initiated for DSC analysis, to be described shortly, a description of a typical catalytic system is provided in the footnote.[1]

2.2 Vacuum assisted resin transfer molding (VARTM)

Vacuum-assisted resin transfer molding (VARTM) is a manufacturing technique used to lower the cost and processing time for fabrication of large scale composite structures (Figure 2.2). VARTM lay-up begins by placing carbon fibers onto an open-faced tool plate. A peelable sheet is then placed over the fibers to facilitate composite removal from the VARTM system after cure. A sheet of resin distribution medium is also commonly used to improve fiber wetting by providing a low resistance resin pathway. Finally, the entire assembly is sealed with a vacuum grade plastic sheet using vacuum tape. After a vacuum is drawn, the catalytic resin system is mixed and the end of the resin distribution tube is submerged into the resin container. The tube valve is then opened to allow the vacuum to pull resin over the fibers. After 24 hours, the VARTM is opened and the composite panels are inspected.

2.3 Differential scanning calorimetry (DSC)

All DSC measurements were performed on a Seiko Instruments 220CU apparatus. The temperature and enthalpy were calibrated using indium and tin standards. All samples included approximately 5 mg of resin. Composite samples also included an additional 5 mg of fiber. All samples were prepared at room temperature and loaded into the DSC,

[1] A common catalytic system involves a peroxide initiator, like M-50 methyl ethyl ketone peroxide (MEKP), and some type of promoter, such as cobalt naphthenate 6% (CoNap). CoNap decomposes the initiating peroxide and as a true catalyst, it is not consumed in the curing reaction. CoNap is a dioctyl phthalate solution that is 6% by weight cobalt. CoNap is initially purple, but turns brown when the transition state of cobalt changes from Co^{2+} to Co^{3+} during decomposition of the initiator.[58] Gel time is controlled by adjusting the proportional amount of initiator and promoter added to the resin. For example, an approximate 30 minute gel time is achieved by using 1.25 phr MEKP and 0.30 phr CoNap with 510A-40 vinyl ester resin. Storing peroxides and vinyl ester resins at cool temperatures is a good way to extend their shelf life.

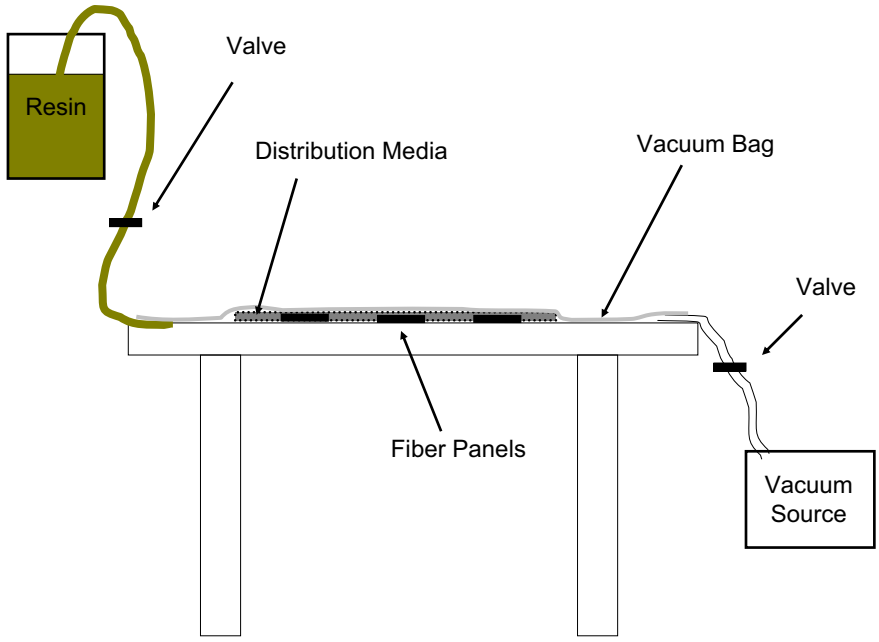

Figure 2.2. Schematic illustration of vacuum-assisted resin transfer molding (VARTM).

held isothermally at 20°C. The DSC was then heated to 350°C at 10°C/min. Results were analyzed using Universal Analysis software and all enthalpy values were normalized to the amount of resin.

2.4 X-ray photoelectron spectroscopy (XPS)

XPS experiments were carried out using a Kratos Axis Ultra XPS system at 10^{-8} torr. The instrument was equipped with a monochromatic Al x-ray source and 15 μm spatial resolution. Fibers were mounted parallel to each other in an aluminum foil packet with a hole cut for analysis. The analyzer was operated in constant analyzer energy mode with a pass energy of 80 eV for broad scans used for elemental quantification and a pass energy of 20 eV for high resolution scans on specific atomic peaks. Intensities were interpreted as elemental concentrations by using sensitivity factors from CasaXPS, the data processing

software package.

XPS is capable of analyzing both chemical composition and chemical state. An important quantity in the discussion of XPS, and later with NEXAFS, is the ionization potential (IP), defined as the minimum energy necessary to excite an electron above the vacuum level. The foundation of XPS analysis is a simple energy balance, shown in Figure 2.3.

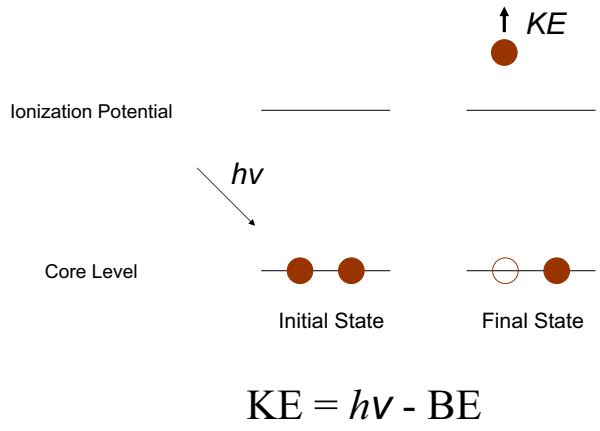

Figure 2.3. Schematic showing the result of X-ray interaction with a material surface in XPS.

First, a photon of known energy (hν) from a fixed energy X-ray source penetrates the surface of a material and is absorbed by a core electron. This core electron is then emitted as a photoelectron with some kinetic energy (KE). If the photoelectron KE is greater than the IP, it escapes the vacuum level and is counted at a detector along with it's KE. The difference between the original photon energy and the recorded photoelectron KE is the binding energy (BE) of that specific core electron. Each electron of an atom has a characteristic BE that is dependent on chemical state.

2.5 Near edge X-ray absorption fine structure (NEXAFS)

NEXAFS measurements were performed at the U7A beamline of the National Synchrotron Light Source at Brookhaven National Laboratory, with the kind assistance of Dr. Robert

Klein. Spectra were collected at room temperature and high vacuum over the region 200 to 750 eV. A monochromator with 600 lines/mm grating provided 0.15 eV resolution. In addition, a retarding adjustable entrance grid bias (V_{bias}) of -150 V was placed across the electron detector in order to screen out Auger electrons with energy less than V_{bias}.

NEXAFS, like XPS, utilizes X-rays to probe the surface for elemental and chemical state information. First pioneered by Stohr, Jaeger, and Outka, NEXAFS most commonly analyzes the K-edges of carbon, nitrogen, and oxygen in the 250 to 750 eV range.[59,60,61] The absorption edge refers to the entire elemental edge, such as the carbon K-edge, and the magnitude of the absorption edge is proportional to the concentration of that atom.

NEXAFS is based on the excitation of electrons from a core level to partially filled and empty states in the same system. When a core electron is excited by a photon, it can be emitted as a photoelectron or excited to a higher energy level. The vacancy at the core level is then filled by an electron from a higher energy level, resulting in the release of a photon. This photon can be emitted as a fluorescent photon or transferred to another electron that is ejected as an Auger electron.

Due to multiple inelastic scattering events, NEXAFS primarily detects secondary electrons, but some Auger electrons, and very few photoelectrons or fluorescent photons. A gate bias is commonly applied to screen out lower velocity electrons. In NEXAFS, the electrons that escape, but are emitted from furthest within the film, are low in energy due to inelastic interactions with other atoms. These low energy electrons may not have enough kinetic energy to pass the negative detector bias and are not detected. The application of a negative detector bias voltage increases surface sensitivity and in this study a gate bias of -150 V was used. The area of a particular NEXAFS peak is proportional to the concentration (or density) of atomic bonding states specific to that peak. The intensities of peaks may be proportional to concentration if the peak widths remain constant. For the most part NEXAFS exhibits good selectivity, but overlap of energy regions does occur. The results were

baselined by linear best fitting a region of relatively constant intensity on the low binding energy side of the absorption edge, followed by normalization to a single point in that same region.

2.6 Attenuated total reflectance - fourier transform infrared spectroscopy (ATR-FTIR)

A Bruker Hyperion 3000 coupled to an Bruker IFS 66/s FTIR spectrometer was used. The objective was a 20x ATR Ge crystal. An MCT detector was used with a resolution of 8 cm^{-1} and up to 1000 scans were done in an attempt to improve the signal to noise ratio.

Chapter 3

Results and Discussion

3.1 DSC

As discussed in the introduction, an important consideration in fiber reinforced polymer composites is the potential for fiber reinforcements to impact resin cure and, consequently, composite performance. In this thesis, the exothermic reaction of neat vinyl ester resin, vinyl ester resin reinforced by neat carbon fibers, and vinyl ester resin reinforced by oxidized carbon fibers was studied with DSC. An important discussion located in Appendix A.1 considers the experimental history that led to the selection of this particular composite system, and describes some of the difficulties encountered during this work.

The initial experimental objective was to investigate potential carbon fiber induced vinyl ester cure inhibition with DSC. These results are displayed in Figure 3.1 and Table 3.1. Both neat and oxidized carbon fibers clearly inhibited vinyl ester polymerization. Further, oxidized carbon fibers induced greater cure inhibition than neat carbon fibers. Evidence of cure inhibition in these data included decreased reaction enthalpy, increased temperature at which peak cure rate occurs, and slower maximum cure rate. Cure rate, as defined in this thesis, is the rate of heat released per unit mass of resin. Several implications can be drawn from these observations. First, since all reaction enthalpies are normalized to resin weight, the decrease in enthalpy is a direct reflection of a lower extent of reaction. Second, the delay in cure exotherm represents a delay in free radical accumulation, a process that

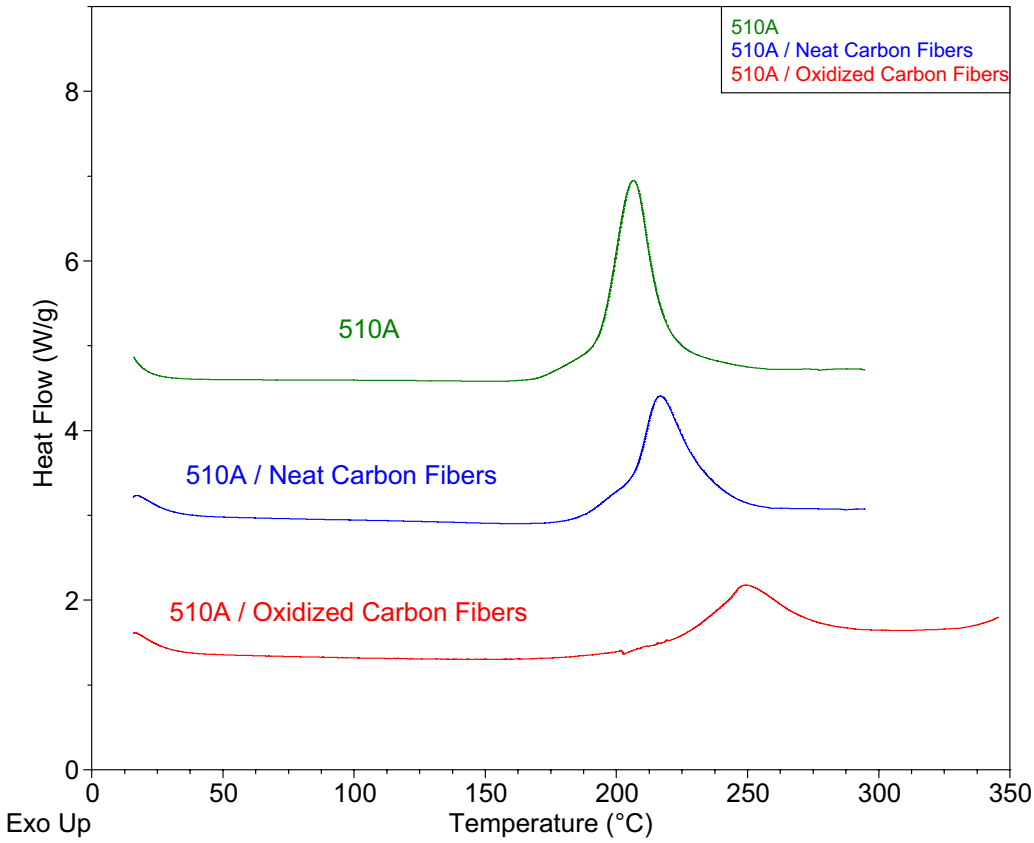

Figure 3.1. Representative cure exotherms for non-isothermal, thermally initiated, 510A-40 vinyl ester resin reinforced by neat and oxidized PAN-based carbon fibers.

occurs when free radical generation surpasses consumption. A similar effect is observed when resin systems are formulated with inhibitors to extend shelf life. Although inhibitors initially slow crosslinking after reaction initiation, their inhibitive effects diminish with time as they are consumed.[16] Third, the decrease in maximum cure rate reflects some limitation on the accumulation of free radicals, since free radical concentration is proportional to cure rate.

Glass transition temperature is an important material property that is related to the degree of cure and overall mechanical properties. Unfortunately, DSC analysis was not able to observe a glass transition in the composite systems. However, a neat vinyl ester Tg of 106°C was identified.

Table 3.1. The DSC data for non-isothermal, thermally initiated, 510A-40 vinyl ester resin reinforced by neat and oxidized PAN-based carbon fibers.

	Enthalpy (J/g-resin)		Peak Cure (C)		
	Average	STDEV	Average	STDEV	Samples
510A	285	16	205	5	4
510A / Neat Carbon Fibers	201	19	217	0	3
510A / Oxidized Carbon Fibers	118	22	253	4	5

In light of these results, two explanations are proposed for the observed inhibition of vinyl ester polymerization by carbon fibers. First, the carbon fiber reinforcements may inhibit vinyl ester polymerization through a phenomenon known as the 'Trommsdorff' or 'gel' effect.[56] By restricting translational mobility of free radicals, the reinforcing fibers may aid radical trapping, depressing polymerization rates and extent of reaction.[52] Oxidative treatments may exaggerate the 'Trommsdorff' effect by increasing the carbon fibers surface roughness, but this effect alone is not sufficient to explain fully the additional inhibition induced by oxidation. It is not plausible that the increase in surface roughness from oxidative treatments would induce an inhibition equivalent to the presence of the fibers themselves.

A second explanation for the observed inhibition is that the carbon fiber surface chemistry interferes with vinyl ester free radical polymerization. An inhibitor of free radical polymerization is a species that scavenges propagating or initiator derived radicals, preventing polymer chain formation. Inhibition occurs when a propagating free radical reacts with another species to produce an inactive polymer chain. Inhibition can also arise when a propagating radical reacts with another species to produce a less reactive radical, a process termed retardation or degradative chain transfer.

Common functional groups known to inhibit free radical polymerization, such as phenols, quinones, and aromatic nitro-compounds could arise on the carbon fiber surface during oxidation.[62,63] Phenols are known to inhibit polymerization by reacting with radicals to form phenoxy radicals, which then scavenge more radicals, or in the case of hydroquinones by

the loss of a hydrogen to form a quinone, itself an inhibitor. Molecular oxygen is another potential inhibitor. The presence of resin-dissolved molecular oxygen may also exacerbate phenolic inhibition by reacting to form the more easily scavenged peroxy radical. Previous studies have reported molecular oxygen induced vinyl ester cure inhibition.[20,64,65] In addition, the activation energy of a resin system, an important factor in controlling chemical reaction rate, has been correlated with surface polarity, surface free energy, and surface oxygen functionality.[32,47,48,52]

In short, DSC analysis was able to demonstrate that carbon fiber reinforcements inhibited vinyl ester resin cure, confirming the inhibition observed macroscopically in the VARTM of carbon fiber reinforced vinyl ester composites. Oxidizing carbon fibers at elevated temperatures was found to significantly increase the inhibitive effect of carbon fibers on vinyl ester resin cure. Evidence of cure inhibition in these data included decreased reaction enthalpy, increased temperature at which peak cure rate occurs, and slower maximum cure rate. Functional groups commonly known to inhibit free radical polymerization, such as phenols and quinones, are likely present on the neat carbon fiber surface, and may become more concentrated with oxidation. The following sections of this chapter analyze the impact of oxidation on the surface chemistry of carbon fibers in light of the vinyl ester cure inhibition observed in DSC, and the inhibition chemistry discussed above.

3.2 XPS

X-ray photoelectron spectroscopy is the primary tool used in this work to characterize the surface chemistry of carbon fibers. In order to determine the atomic makeup of the carbon fiber surface, a broad XPS survey scan was done and the spectra are shown in Figure 3.2. Table 3.2 provides the reference and experimental electron binding energy peaks that were used to identify specific elements present on the carbon fiber surface.[66] Relative sensitivity

factors (RSFs) were utilized to convert photoelectron intensities into atomic concentrations and the results are reported in Table 3.3. In order to confirm the presence of low concentration elements, a higher resolution survey scan of lower binding energies was done and these spectra are shown in Figure 3.3.

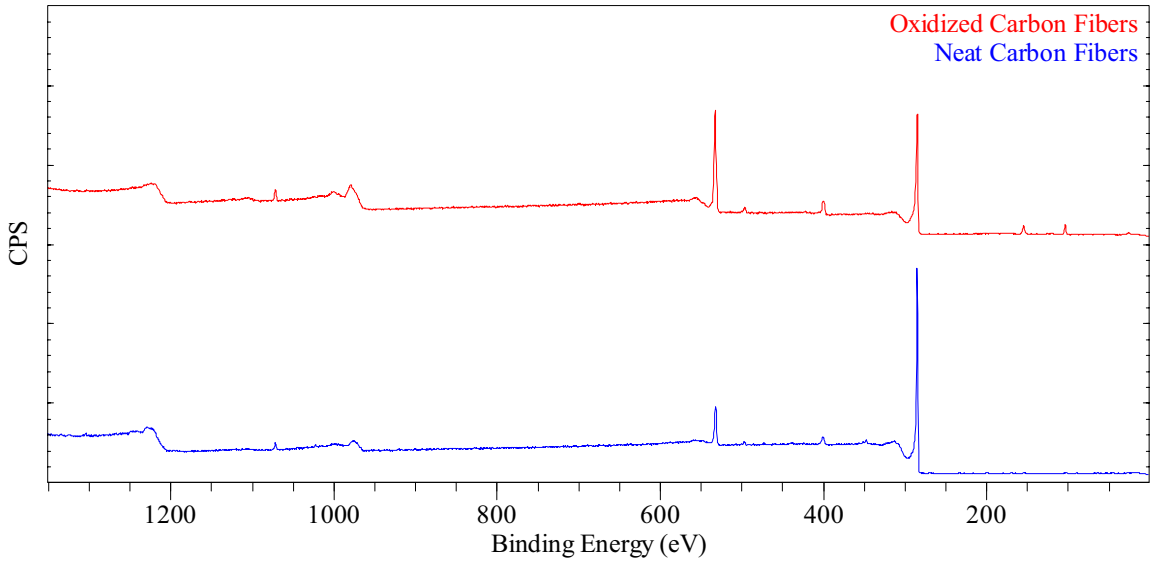

Figure 3.2. The XPS broad survey spectra of neat and oxidized carbon fibers.

As expected, the surface oxygen content increased with oxidation from 7.6 to 19.9 atomic %, while the surface carbon atomic concentration decreased from 88.7 to 69.8 atomic %. Surface nitrogen concentration was observed to increase from 2.4 to 5.6 atomic %. Surface silicon increased from 0.4 to 4 atomic % and surface sodium from 0.2 to 0.6 atomic %. Finally, trace amounts of chlorine, sulfur, magnesium and calcium appeared on the neat carbon fiber surface, but they did not appear after oxidation. These trace elements have been previously reported and have been attributed to supplier production, treatment, and handling processes.[3,8,13,39,40,67] The increase in silicon and sodium concentration may have resulted from absorption of species in the laboratory environment, an effect enhanced by oxidation, which increases surface absorbtivity. Another explanation is that a concentration gradient existed, so that oxidation exposed the more concentrated bulk. This explanation would also

Table 3.2. X-ray Photoelectron Spectrocopy Peak Identification

			Binding Energy Peak (eV)	
Element	Electron	Reference	Neat Carbon Fibers	Oxidized Carbon Fibers
C	1s	285	285	285
O	1s	531	532	533
N	1s	398	401	400
Si	2s	151	153	155
	2p	99	102	104
Na	1s	1072	1072	1072
	2s	64	64	64
	2p	31	30	31
Ca	2s	440	440	-
	2p	351/347	348	-
	3s	45	45	-
	3p	26	26	-
Cl	2s	271	270	-
	2p	201/199	198	-
Mg	1s	1303	1304	-
S	2s	228	234	-
	2p	165/164	169	-

Table 3.3. The relative elemental surface concentrations derived from the XPS broad survey spectra of neat and oxidized carbon fibers.

	Surface Elemental Concentration (Atomic %)	
	Neat Carbon Fibers	Oxidized Carbon Fibers
C	88.7	69.8
O	7.6	19.9
N	2.4	5.6
Si	0.4	4.2
Na	0.2	0.6
Ca	0.4	-
Cl	0.1	-
Mg	0.1	-
S	0.1	-

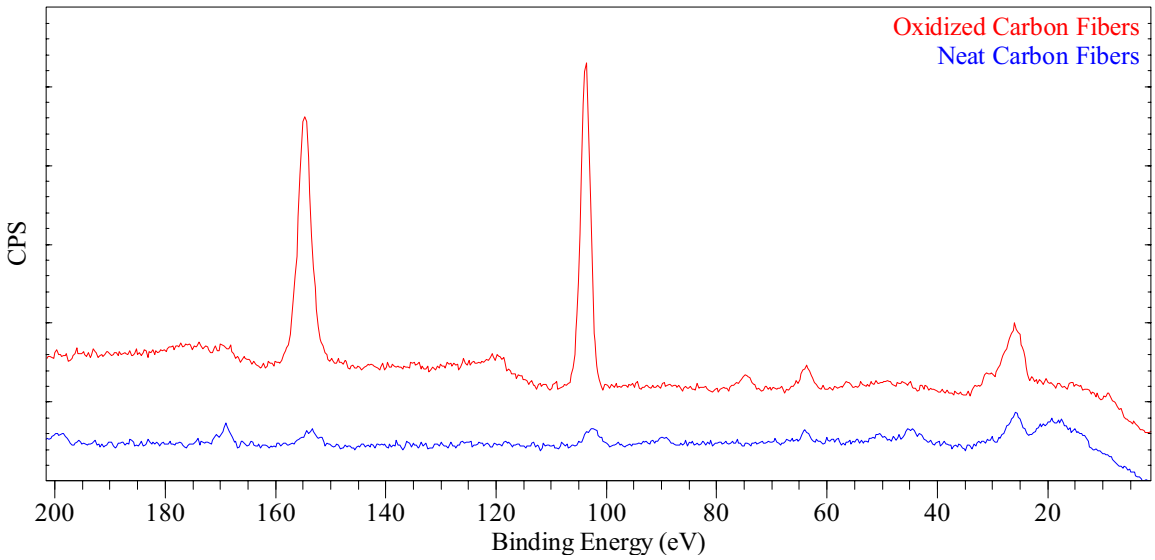

Figure 3.3. The XPS low binding energy survey spectra of neat and oxidized carbon fibers.

explain the loss of several trace elements with oxidation. Since oxidation removes the carbon fibers' outer layers, it would also remove any elements present only on the surface. Overall, these results were consistent with previous work on PAN-based carbon fiber oxidation.[63]

In addition to elemental analysis, XPS is capable of identifying changes in surface chemical structure. A high resolution C 1s scan of neat and oxidized carbon fiber was done for this purpose, and the spectra are shown in Figure 3.4. Oxidation clearly reduced the C 1s peak intensity, confirming the relative decrease in surface carbon identified in the broad survey scan. Furthermore, compared to neat carbon fibers, the C 1s spectrum for oxidized carbon fibers exhibited a slight increase in asymmetry toward higher binding energy, indicating an increase in the concentration of oxidized carbon atoms. However, the asymmetry of the oxidized carbon fiber spectrum was somewhat less than expected, given the previously noted large increase in surface oxygen. One explanation for this is that most of the additional surface oxygen formed single bonds with carbon. In general, the photoelectron binding energy of a C 1s electron increases 1.5 eV per carbon-oxygen bond, and so carbon-oxygen single bonding would produce less asymmetry.[2,42,68,69,70]

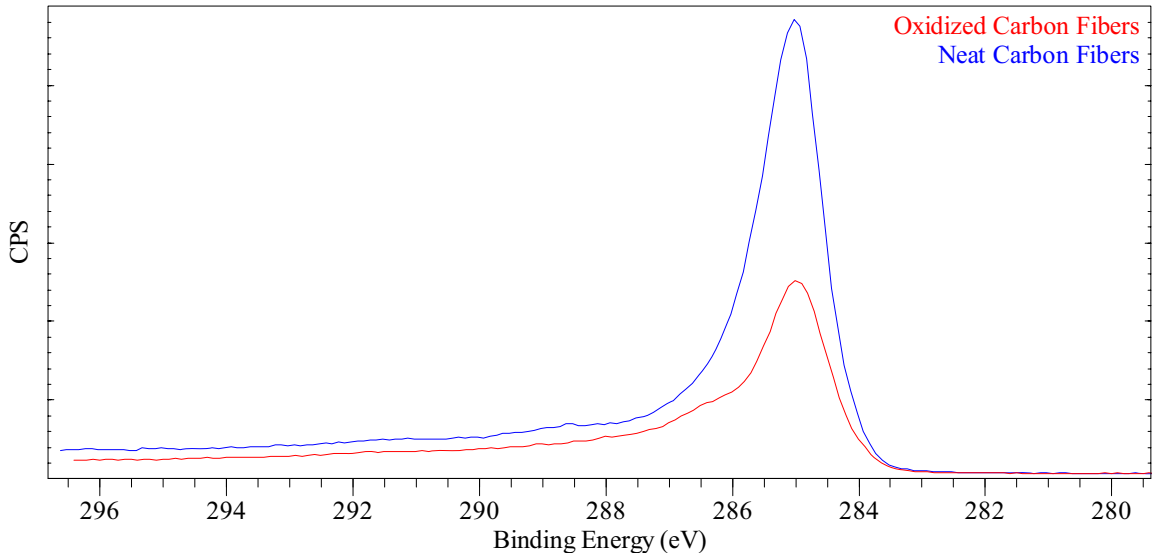

Figure 3.4. The high resolution C 1s spectra of neat and oxidized carbon fibers.

Another explanation for the limited asymmetry is the formation of hydrogen-bridged structures (HBSs). These structures occur when a carbonyl oxygen interacts with the hydrogen of a hydroxyl group, creating two hybrid oxygen atoms with binding energies somewhere between a pure hydroxyl or carbonyl oxygen.[71,72] Finally, some of the increased surface oxygen may be bound to silicon in the form of surface oxides. An important point to keep in mind is that changes in bond polarity do not uniformly impact the binding energy of each atom's electrons. For example, in carbon-oxygen bonding an increase in bond polarity would increase the binding energy of carbon electrons, but would decrease the binding energy of oxygen electrons.

To quantify these changes in surface structure, curve fitting techniques have been developed.[70,73] For calibration purposes, XPS spectra were shifted so that the electron binding energy of graphitic carbon was positioned at 285 eV. Curve fitting was then carried out using a nonlinear least-squares program with a Gaussian/Lorentzian product function. The Gaussian/Lorentzian mix was 0.5, except for the 'graphitic' carbon peak, which used 0.84.[70] The spectra were then fit by a main 'graphitic' peak around 285 eV and three energy con-

strained 'oxide' peaks. Each functional group was constrained within the broadest range of binding energies found in the literature and these constraints are presented in Table 3.4. The full width half max (FWHM) for each oxide peak was set equal to the FWHM of the 'graphitic' peak and the resulting relative concentrations of C 1s chemical states are presented in Table 3.5. While C-C bonding decreased by 6 %, O-C=O bonding increased 1.3 %, C=O bonding increased 2.0 %, and C-O bonding increased 2.8 %. The functional groups in Table 3.5 show only carbon-oxygen bonding, but since nitrogen and oxygen have similar electronegativities they have a similar effect on the binding energies of carbon bound electrons.

Table 3.4. The binding energies used to constrain the oxide peaks in curve fitting the C 1s spectra.[1,2,3,4]

Functionality	Binding Energy Shift (eV)
C-OH, C-O-C	1.13 - 1.75
C=O	2.90 - 3.10
COOH, COOR	3.64 - 4.50

Table 3.5. Results of curve fitting the C 1s spectra of neat and oxidized carbon fibers.

	Surface Functional Concentration (Atomic %)	
	Neat Carbon Fibers	Oxidized Carbon Fibers
C - C	79.3	73.2
C - O	11.3	14.1
C = O	5.7	7.7
O - C = O	3.7	5.0

High resolution O 1s and N 1s scans were done to provide further analysis of changes in carbon fiber surface chemistry due to oxidation, but curve fitting these peaks is less well defined, so only qualitative changes will be discussed. A high resolution O 1s scan was conducted for neat and oxidized carbon fibers and the spectra are shown in Figure 3.5. The significant intensity increase in the O 1s of oxidized carbon fiber confirmed the large increase

in surface oxygen observed in the broad survey scan. The O 1s spectra exhibited two primary features. The first feature, at 533 eV, corresponds to hydroxyl and ether oxygens (-OH and -R-O-R-). The second feature, at 531.5 eV, corresponds to carbonyl oxygens (=O).[3,68,71,72] After oxidation, the O 1s spectrum exhibited a dramatic increase in the amount of σ-bonded oxygen. Although carbon-oxygen double bonds contain both π-electrons and σ-electrons, carbon-oxygen single bonds have only σ-electrons. Therefore, not all of the additional σ-bonding is attributable to single bonds. Overall, the O 1s spectra were consistent with the C 1s spectra. Both demonstrated that oxidation increased the concentration of surface oxygen atoms, primarily in σ-bonding.

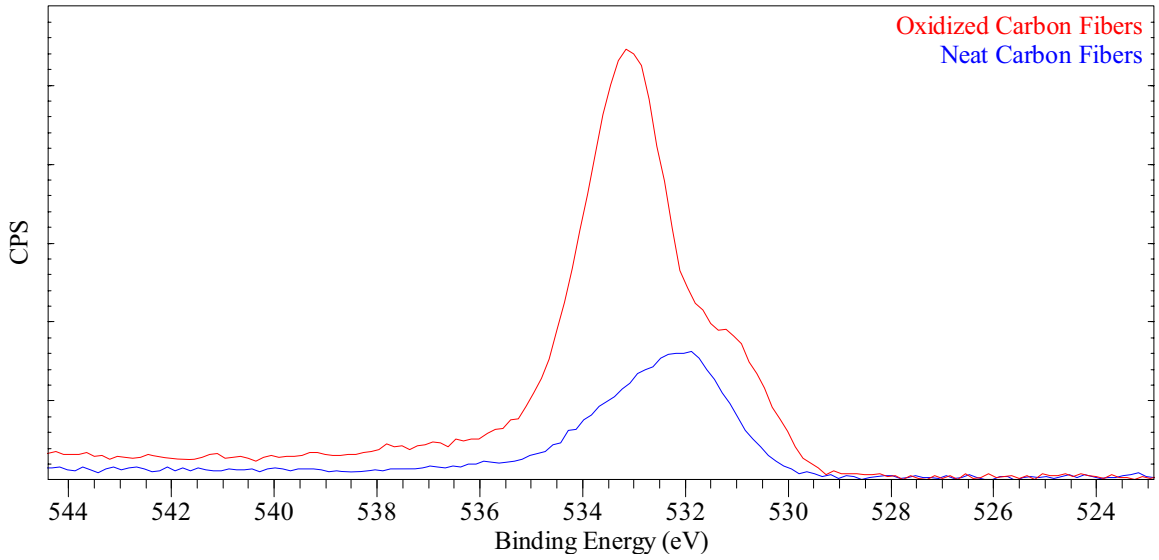

Figure 3.5. The high resolution O 1s spectra of neat and oxidized carbon fibers.

A high resolution N 1s scan was also done for neat and oxidized carbon fibers, and the spectra are shown in Figure 3.6. The intensity increase of the high resolution N 1s spectrum of oxidized carbon fibers also confirmed the broad survey spectra elemental analysis. The increase in surface nitrogen after oxidation is either the result of exposing a more nitrogen rich bulk or from reaction with an atmospheric nitrogen species. Given that the production of carbon fibers involves heat treatment under nitrogen at temperatures up to 1500°C to

drive off non-carbon atoms, diatomic nitrogen in air is unlikely to be the source. No other nitrogen species are present in air at significant enough concentrations to explain the increase in surface nitrogen observed after oxidation. The observed increase in surface nitrogen must then derive from the bulk. Previous studies have reported a concentration gradient due to residual PAN nitrogen with increasing concentration toward the bulk.[74,75] Since oxidation exposes the more nitrogen rich bulk, it would result in a more nitrogen rich surface.

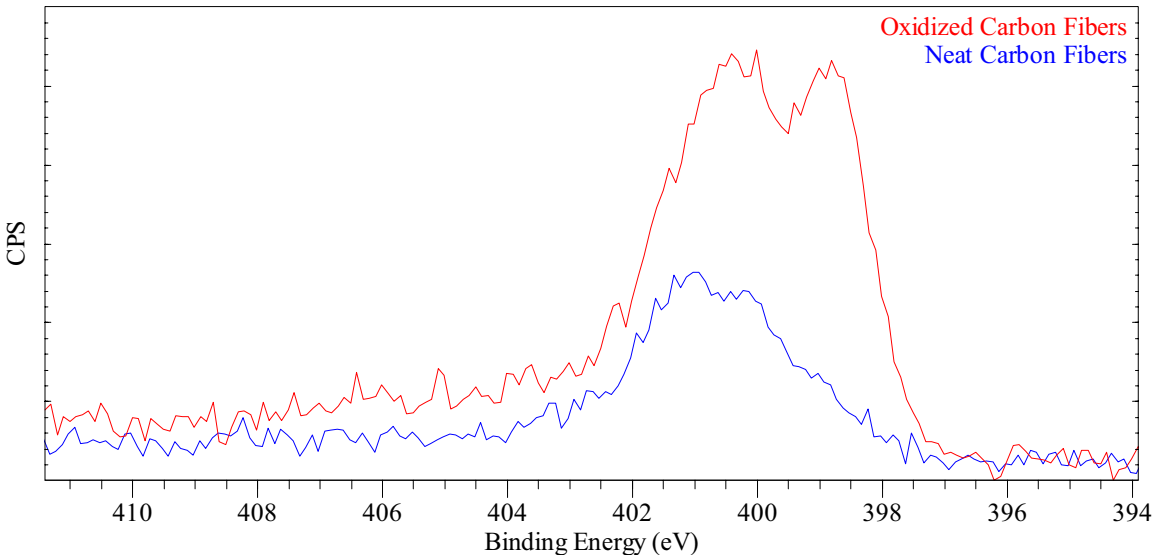

Figure 3.6. The high resolution N 1s spectra of neat and oxidized carbon fibers.

The N 1s spectra exhibited two key structural features. The first feature, at 401-402 eV, was attributed to oxidized nitrogen, nitrogen bound to carbonyls, and quaternized nitrogen. Quaternized nitrogen is nitrogen with a fourth attached group that induces a formal positive charge. Another feature, at 399 eV, was considered to represent non-quaternized nitrogen.[2,4,76,77] While oxidation clearly increased the intensity at 401 eV, the increase at 399 eV was even more dramatic. Therefore, while most nitrogen in neat carbon fibers was oxidized or quaternized, after oxidation an almost equal amount of each feature was present.

In summary, an XPS broad survey scan established the atomic surface chemistry for neat and oxidized carbon fibers. Oxidized carbon fibers demonstrated a significant increase in

surface oxygen and surface nitrogen atomic concentration, and a corresponding decrease in surface carbon atomic concentration. Trace amounts of Si, Na, Ca, Cl, Mg, and S were observed on the neat carbon fiber, but only Si and Na remained after oxidation, increasing slightly. High resolution XPS scans of carbon, oxygen, and nitrogen confirmed the broad survey scan results and provided a more detailed analysis of carbon fiber surface functionality. The high resolution carbon spectra for oxidized carbon fiber showed a slight increase in asymetry compared with spectra for neat carbon fibers, indicative of an increase in carbon bound to either oxygen or nitrogen. The high resolution oxygen spectra showed a moderate increase in binding energy at 531.5 (carbonyl oxygens), and a large increase at 533 eV (hydroxyl or ether oxygens). The high resolution nitrogen spectra demonstrated a moderate increase in binding energy at 401.5 eV (oxidized nitrogen, nitrogen bound to carbonyls, and quaternized nitrogen), and a larger increase at 399 eV (non-quaternized nitrogen).

3.3 NEXAFS

NEXAFS is a much more recently developed technique than XPS, but it offers the potential for a more detailed characterization of surface functionality. As described in Chapter 2, NEXAFS most commonly analyzes the K-edges of carbon, nitrogen, and oxygen in the 250 to 750 eV range.[59,60,61]

The C K-edge spectra are presented in Figure 3.7. The first feature, at 285 eV, was attributed to a strong π-transition arising from unsaturated carbon atoms, likely aromatic carbons. The 287 eV feature clearly increased with oxidation and was attributed to the presence of hydroxylated aromatic carbons (phenols) and carbonyl carbons.[78,79,80] The feature at 288.5 was assigned to carboxylic acids, and the feature at 292 eV was attributed to the σ-bonding of aromatic carbon.[81] The most apparent effect of oxidation on the C K-edge spectra was to increase absorption around 287 eV. This observation suggests an increase

in locally bound surface oxygens, since aromatic carbons bound to or near oxygens atoms are understood to become slightly electron deficient, shifting their π-resonance to higher energy.[79]

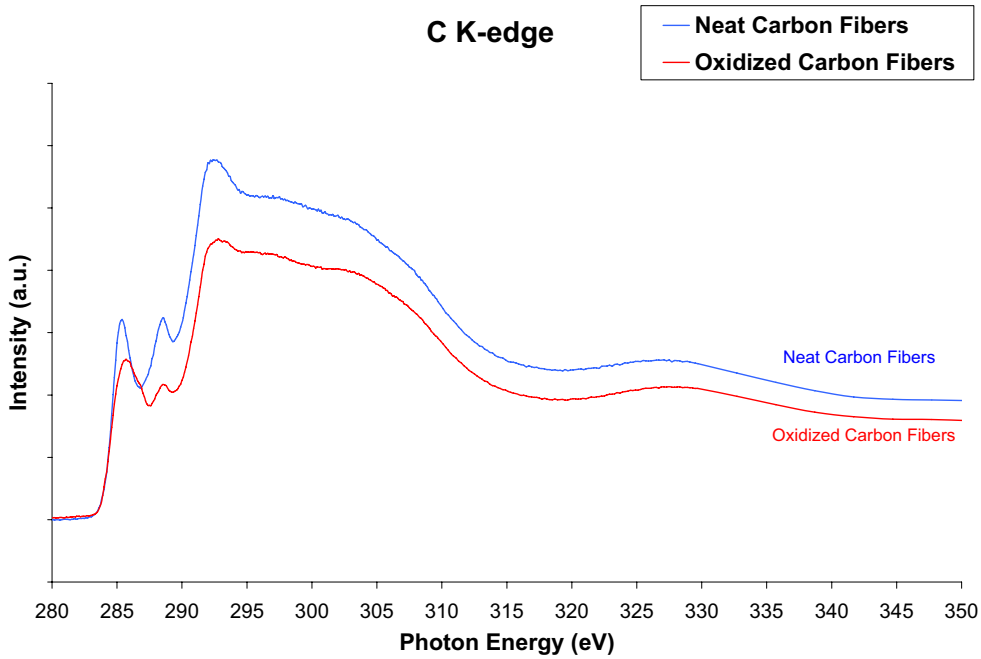

Figure 3.7. NEXAFS spectra of the carbon K-edge of neat and oxidized carbon fibers.

The O K-edge spectra, shown in Figure 3.8, exhibited two primary features. The feature at 534 eV was assigned to π-bonded oxygens, and the feature at 541 eV to σ-bonded oxygens. Oxidized carbon fiber showed only a slight increase in π-bonded oxygen, but a rather dramatic increase in σ-bonded oxygen. Finally, a shift in the π-bonded oxygen feature to higher energies is observed.

The N K-edge spectra, shown in Figure 3.9, exhibited two primary features. The first feature, at 402 eV, was assigned to π-bonded nitrogen, possibly due to pyridone functionality

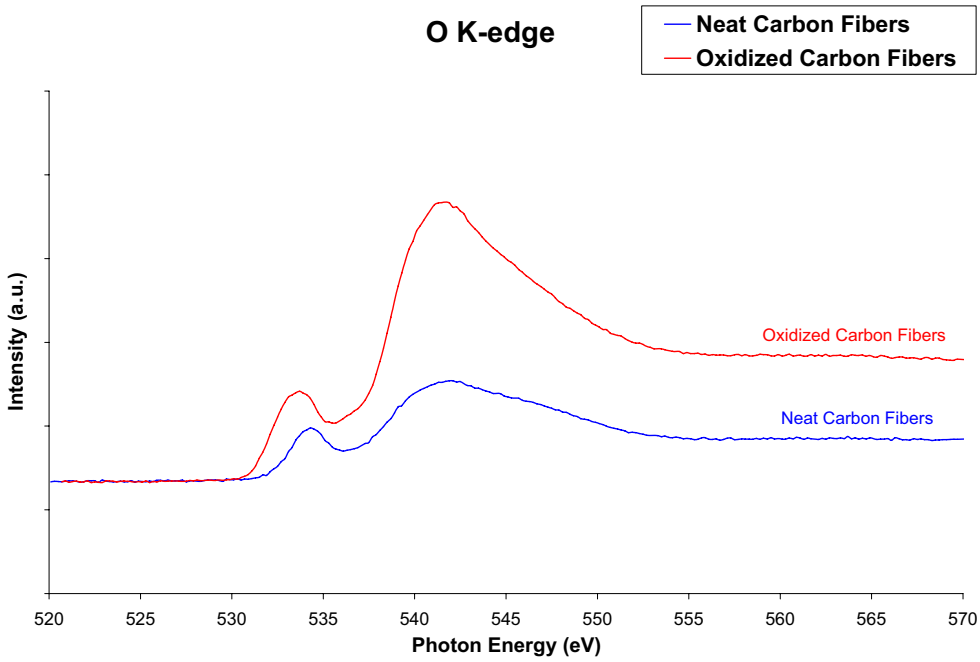

Figure 3.8. NEXAFS spectra of the oxygen K-edge of neat and oxidized carbon fibers.

arising from surface oxidation.[82] The second feature, at 408 eV, was assigned to σ-bonding from either aromatic nitrogens or saturated amines.[82,83] Oxidation produced a large absorption increase at 402 eV, indicating additional π-bonded nitrogens were introduced to the carbon fiber surface.

Overall, NEXAFS supported the conclusions drawn from XPS analysis. Similar to XPS spectra, NEXAFS spectra suggested an increase in the amount of locally bound surface oxygen and nitrogen after oxidation. The C K-edge spectra exhibited an increase in the 287 eV binding energy peak, which is indicative of hydroxylated aromatic carbons and carbonyl carbons. The N K-edge spectra showed a greater increase in π-bonded nitrogen than σ-bonded nitrogen. The O K-edge spectra indicates a slight increase in π-bonded oxygen after

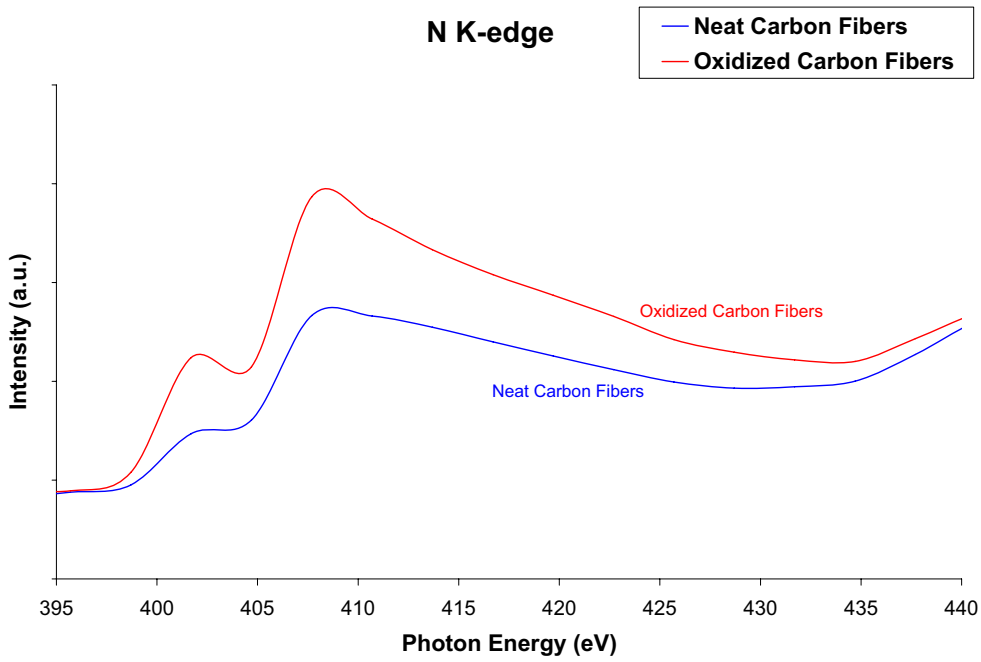

Figure 3.9. NEXAFS spectra of the nitrogen K-edge of neat and oxidized carbon fibers.

oxidation, but a rather dramatic increase in σ-bonded oxygen, further evidence for hydroxyls and carbonyls.

3.4 ATR-FTIR

ATR-FTIR was conducted on both neat and oxidized carbon fibers and the spectra are shown in Figure 3.10. Unfortunately, characterization of carbon via FTIR is problematic, mostly due to an intense background absorption. As expected, initial ATR-FTIR spectra exhibited a the broad absorption background that complicates FTIR analysis of carbonaceous materials. However, it was found that by removing the sample and capturing spectra of the residual material that higher resolution spectra could be achieved. Very little absorption

was observed in the spectra of residual neat fiber material, possibly because the surface of neat fiber is less brittle, and so less material would be left on the ATR crystal for analysis.

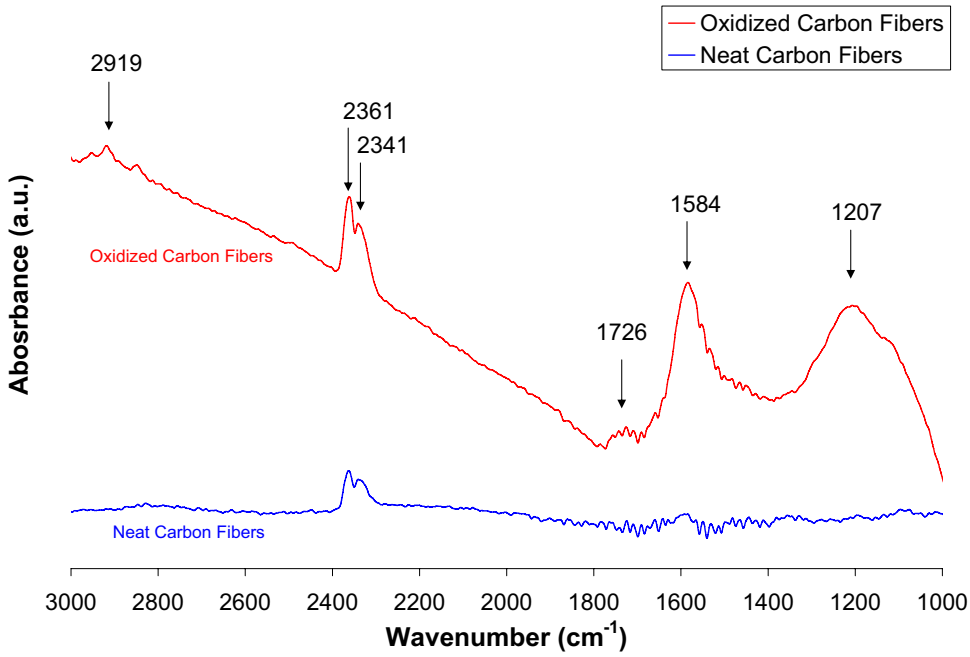

Figure 3.10. ATR-FTIR spectra of neat and oxidized carbon fibers.

The absorption band at 1207 cm^{-1} is associated with C-O stretching and O-H bending modes in functional groups with σ-bonding characteristics, such as phenols.[84,85,86] Assignment of the 1584 cm^{-1} band is uncertain due to some remaining controversy. The two most probable assignments of this band are aromatic ring stretching or highly conjugated, hydrogen bonded carbonyl groups. Evidence supporting the assignment of this band to aromatic ring stretching has been presented by Painter, et al. in a number of publications.[84,85,86] In their previous analysis of oxidized coal, a 1585 cm^{-1} band was assigned to aromatic ring stretching, and it was observed that this band was enhanced by oxygen containing functional

groups resulting from oxidation.[86] The absorption band observed at 1726 cm^{-1} is characteristic of carbonyl groups. An analysis of oxidized coal by Painter, et al. assigned a similar band at 1720 cm^{-1} to carbonyl vibrations in carboxylic acid groups. The features at 2341 and 2361 cm^{-1} are likely the result of CO_2 and should be ignored. Finally, the band at 2920 cm^{-1} is characteristic of CH, CH_2 and CH_3 groups attached to aromatic units.[85,86]

ATR-FTIR analysis is a difficult technique for the study of carbon fibers. Nevertheless, these results did support the general notion that oxidation increased the amount of surface bound oxygen and nitrogen. The spectrum for oxidized carbon fibers demonstrated a strong feature at 1726 cm^{-1}, evidence supporting the presence of surface oxygen, specifically carbonyl groups. Additionally, the feature at 1584 cm^{-1} is likely aromatic ring stretching enhanced by oxygen containing functional groups. Finally, the feature at 1207 cm^{-1} is characteristic of C-O stretching and O-H bending modes, further supporting the presence of hydroxyls, and possibly phenols.

Chapter 4

Summary and Suggestions for Future Work

4.1 Summary

Carbon fiber reinforced polymer composites offer impressive specific properties and significant application potential. Unfortunately, structures composed of carbon fiber reinforced vinyl ester resins have failed at lower stress levels than expected, specifically under transverse loading. These problems are thought to arise from poor fiber-matrix adhesion, but research to improve adhesion by adjusting fiber surface properties has produced limited and unsatisfactory progress. The motivation for this thesis developed when a VARTM of vinyl ester resin reinforced by oxidized carbon fibers resulted in structures with properties indicative of cure inhibition.[6,87] The intention of this thesis was to confirm the macroscopically observed inhibition with DSC, and then to investigate the carbon fiber surface chemistries that may be responsible with XPS, NEXAFS, and ATR-FTIR. It was thought that functional groups commonly known to inhibit free radical polymerization, such as phenols and quinones, may be present on the neat fiber surface, and may become more concentrated through oxidation.

DSC results confirmed that neat carbon fibers, and to an even greater extent oxidized carbon fibers, inhibited the cure of vinyl ester resin. Evidence of cure inhibition in these data included decreased reaction enthalpy, increased temperature at which peak cure rate occurs, and slower maximum cure rate. Although the 'Trommsdorff' effect could be a contributing factor to inhibition, this effect alone is not sufficient to explain the additional inhibition

induced by oxidation.

Surface characterization via XPS established the elemental surface chemistry of neat and oxidized carbon fibers. The broad survey spectra of neat and oxidized carbon fibers identified carbon, oxygen, and nitrogen atoms, as well as several trace elements, including Ca, Cl, Mg, S, Si, and Na. Of these trace elements, all but Si and Na were eliminated by oxidation, indicating that they existed only in the outer layers of neat carbon fibers. Conversely, silicon and sodium content increased with oxidation, a result attributed to a gradient of increasing concentration into the bulk. Similarly, oxidation produced a greater surface concentration of nitrogen, thought to be due to a gradient of residual nitrogen from the PAN precursor remaining in the bulk. As expected, oxidation decreased surface carbon content and increased the surface oxygen content. High resolution XPS, NEXAFS, and ATR-FTIR were then used to provide a more detailed analysis of the neat carbon fiber surface chemistry and the effect of oxidation.

The C 1s spectrum for oxidized carbon fibers exhibited only a slight increase in asymmetry toward higher binding energies, evidence that a large amount of the additional oxygen was bound to carbon as hydroxyls or ethers. The O 1s spectrum supported this conclusion, with oxidation producing a substantial increase in hydroxyl or ether functionality, but only a moderate increase in carbonyl functionality. The O K-edge spectra produced yet more evidence for additional surface bound oxygen atoms resulting from oxidation, with some π-bonding, but mostly σ-bonding characteristics. These results further supported the conclusion that oxidation added some carbonyls, but mostly hydroxyls or ethers. The C K-edge spectra for oxidized carbon concured, with evidence for additional hydroxylated aromatic carbons and carbonyl carbons. From the N 1s and N K-edge spectra, it is clear that most of the additional nitrogen is non-quaternized and π-bonded. Finally, ATR-FTIR spectra supported a general increase in carbon-oxygen bonding after oxidation, demonstrating an increase in features characteristic of C-O stretching, O-H bending, and carbonyl groups.

Taken together, these results clearly support the conclusion that carbon fiber oxidation increased the amount of oxygen atoms bound to the carbon fiber surface, mostly as hydroxyls or ethers, but also as carbonyls. These functional groups are present on common inhibitors of free radical polymerization, such as phenols and quinones, and their presence on the carbon fiber surface is likely the cause of vinyl ester cure inhibition observed with DSC.

4.2 Suggestions for Future Work

The desired end of this work, and any future work, is ultimately to realize the full application potential of carbon fiber reinforced vinyl ester by improving their performance. The path to success likely includes the introduction of a chemical treatment step to the carbon fiber production process that eliminates any surface functionalities responsible for cure inhibition. Future work should confirm the functional groups present on both neat and oxidized carbon fiber surfaces. One method to achieve this is through the application of chemical markers in conjunction with characterization techniques. Once specific surface functional groups are confirmed, the next effort should be to systematically eliminate each functionality from the carbon fiber surface via chemical reaction, followed by analysis with DSC. If the removal of a functional group eliminates the inhibitive effect of carbon fiber on vinyl ester, then the functionality responsible for poor fiber-matrix adhesion has likely been identified. An alternative method to identifying the responsible functionality would be to systematically introduce each suspect functional group to the fiber surface, followed by DSC analysis to evaluate their impact on vinyl ester cure. Once the presence of specific functionalities is confirmed, neat woven carbon fibers should be reacted in a similar manner prior to panel fabrication via VARTM. In theory, composites fabricated from these treated carbon fibers and vinyl ester resin will yield more robust properties.

Another set of experiments could investigate the relationship between the degree of oxida-

tion and the extent of cure inhibition to establish a correlation between oxidation conditions and vinyl ester cure inhibition. Investigating the impact of neat and oxidized carbon fibers on the polymerization of non-brominated vinyl esters, epoxy resins, and polyester resins would also be interesting.

Appendix A

Preliminary Experimental Results

A.1 Discussion of Preliminary Experimental Results

Almost all commercially produced vinyl ester composite systems utilize sized fibers and a catalytically initiated resin system. Sizing facilitates processing and improves fiber-matrix adhesion, while a catalytically initiated system enables room temperature cure and reduces production costs. Therefore, in order to use the most practical composite system, initial experiments were conducted with sized fibers and a catalytically initiated system. Despite the apparent cure inhibition observed in VARTM trials, no statistically significant cure inhibition was observed in either the isothermal or non-isothermal DSC analysis of vinyl ester resin reinforced with sized carbon fibers that had been oxidized (See Appendix A: Figure A.1 and A.2; Table A.1 and A.2). Surprisingly, vinyl ester cure was actually promoted by the presence one sample of sized carbon fibers that had been oxidized.

After observing these inconclusive and contradictory results, and given the proprietary nature of the sizings, a decision was made to simplify the system by using unsized carbon fibers. Finally, VARTM and isothermal DSC analysis demonstrated clear cure inhibition.(Appendix A: Figure A.3 and Table A.3) Unfortunately, vinyl ester reinforced by neat unsized fibers suffered from significant variability in both enthalpy and time to max cure rate. A significant effort was invested to control the timing of each process step, a critical parameter in free radical polymerization. Other potentially significant variables such as ambient temperature, humidity, fiber loading level, and very slight variations in promoter and initiator concentration were recorded, but were not found to correlate with the exotherm variability. Therefore, the system was further simplified, this time by eliminating the promoter and initiator, a helpful suggestion provided by Eric Strauch (ARL Penn State). Finally, DSC analysis of thermally initiated vinyl ester reinforced by unsized fibers exhibited consistent

DSC results with clear inhibition due to carbon fiber oxidation. These results are displayed in Figure 3.1 and Table 3.1.

A.2 Preliminary Experimental Results

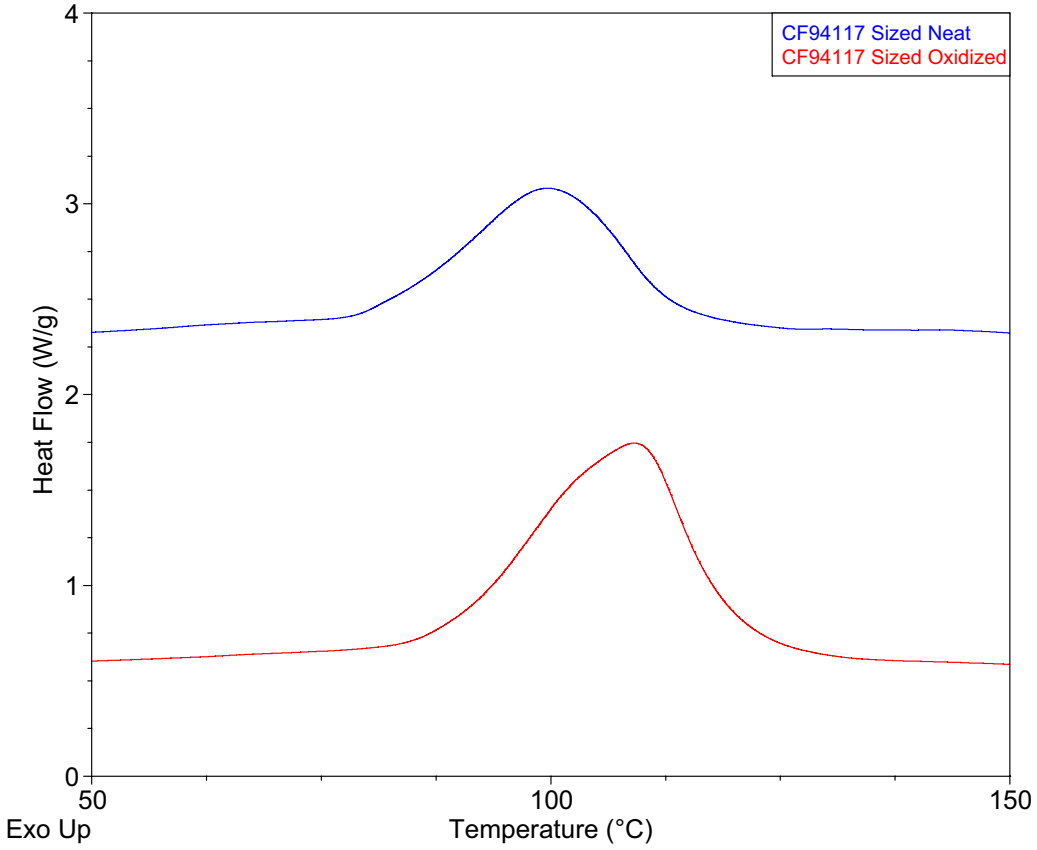

Figure A.1. Representative cure exotherms for non-isothermal 510A-40 vinyl ester resin, initiated by 1.25 phr M-50 MEKP, promoted by 0.3 phr CoNap (6% cobalt), and reinforced by neat and oxidized sized PAN-based carbon fibers.

Table A.1. Cure exotherm data for non-isothermal 510A-40 vinyl ester resin, initiated by 1.25 phr M-50 MEKP, promoted by 0.3 phr CoNap (6% cobalt), and reinforced by neat and oxidized sized PAN-based carbon fibers.

	Enthalpy (J/g-resin)		Peak Cure (C)		
	AVG	STDEV	AVG	STDEV	Samples
510A	228	10	120	2	6
510A / Sized Carbon Fibers (neat)	244	31	102	6	6
510A / Sized Carbon Fibers (oxidized)	298	19	106	4	4

Table A.2. Cure exotherm data for the 50°C isothermal cure of 510A-40 vinyl ester resin, initiated by 1.25 phr M-50 MEKP, promoted by 0.3 phr CoNap (6% cobalt), and reinforced by neat and oxidized sized PAN-based carbon fibers.

	Enthalpy (J/g-resin)	Peak Cure (minutes)
510A / Sized 94117 (neat)	210	65
510A / Sized 94117 (oxidized)	170	110
510A / Sized 94933 (neat)	164	75
510A / Sized 94933 (oxidized)	192	90

Table A.3. Cure exotherm data for the 50°C isothermal cure of 510A-40 vinyl ester resin, initiated by 1.25 phr M-50 MEKP, promoted by 0.3 phr CoNap (6% cobalt), and reinforced by neat and oxidized unsized PAN-based carbon fibers.

	Enthalpy (J/g-resin)		Peak Cure (minutes)		
	Average	STDEV	Average	STDEV	Samples
510A / Neat Carbon Fibers	150	51	161	53	4
510A / Oxidized Carbon Fibers	-	-	-	-	4

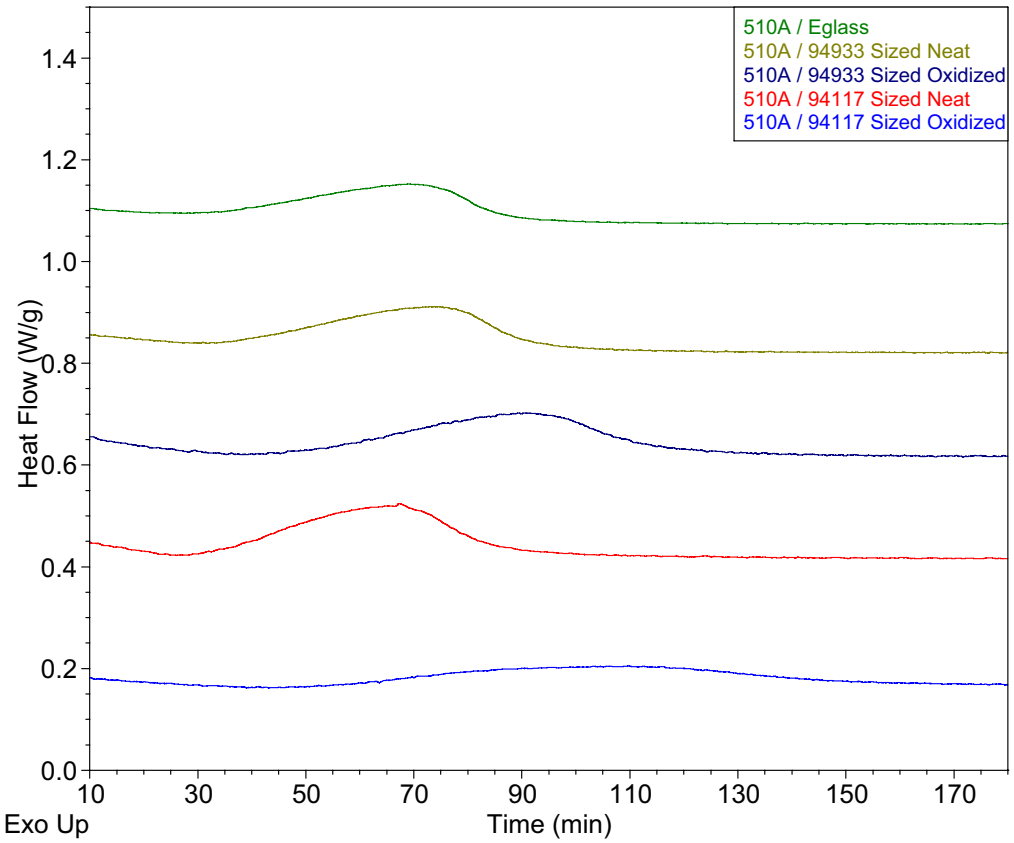

Figure A.2. Representative cure exotherms for the 50°C isothermal cure of 510A-40 vinyl ester resin, initiated by 1.25 phr M-50 MEKP, promoted by 0.3 phr CoNap (6% cobalt), and reinforced by neat and oxidized sized PAN-based carbon fibers.

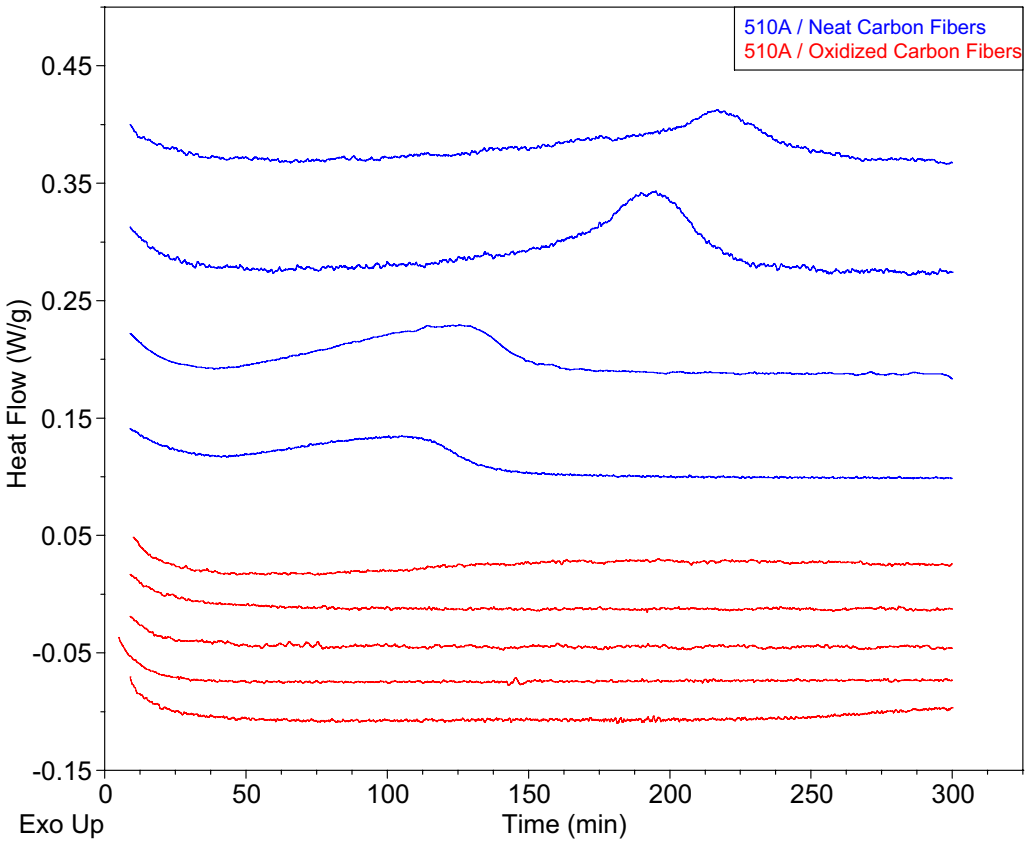

Figure A.3. Representative cure exotherms for the 50°C isothermal cure of 510A-40 vinyl ester resin, initiated by 1.25 phr M-50 MEKP, promoted by 0.3 phr CoNap (6% cobalt), and reinforced by neat and oxidized unsized PAN-based carbon fibers.

List of References

1. Dilsiz, N. and Wightman, J. P. Surface analysis of unsized and sized carbon fibers. *Carbon* **37**(7), 1105–1114 (1999).

2. Lee, W. H., Lee, J. G., and Reucroft, P. J. XPS study of carbon fiber surfaces treated by thermal oxidation in a gas mixture. *Applied Surface Science* **171**(1-2), 136–142 (2001).

3. Weitzsacker, C. L., Xie, M., and Drzal, L. T. Using XPS to investigate fiber matrix chemical interactions in carbon-fiber-reinforced composites. *Surface And Interface Analysis* **25**(2), 53–63 (1997).

4. Beamson, G. and Briggs, D. *High Resolution XPS of organic polymers: the Scienta ESCA300 database*. Wiley, New York, (1992).

5. Barsoum, R. G. S. Navy experts explain the newest material and structural technologies. *AMPTIAC Quarterly* **7**(3), 55–61 (2003).

6. Juska, T. Effect of Water Immersion on Fiber/Matrix Adhesion. Technical report, Ship Materials Engineering Department, Carderock Division, Naval Surface Warfare Center, (1993).

7. Sherwood, P. M. A. Surface analysis of carbon and carbon fibers for composites. *Journal Of Electron Spectroscopy And Related Phenomena* **81**(3), 319–342 (1996).

8. Rich, M. J. and Drzal, L. T. Interphase properties of carbon fiber-vinyl ester composites. In *Advanced Composites Conference*, 463–473, (1997).

9. Xu, L. and Drzal, L. T. Influence of interphase chemistry on the adhesion between vinyl ester resin and carbon fibers. In *Proc. Annu. Meet. Adhes. Soc.*, volume 23, (2000).

10. Kim, I. C. and Yoon, T. H. Enhanced interfacial adhesion of carbon fibers to vinyl ester resin using poly(arylene ether phosphine oxide) coatings as adhesion promoters. *Journal Of Adhesion Science And Technology* **14**(4), 545–559 (2000).

11. Jones, C. The chemistry of carbon-fiber surfaces and its effect on interfacial phenomena in fiber epoxy composites. *Composites Science And Technology* **42**(1-3), 275–298 (1991).

12. Xu, L. and Drzal, L. T. International conference on composite materials. In *13th International Conference on Composite Materials*, (2001).

13. Drzal, L. T. and Bascom, W. D. The surface properties of carbon fibers and their adhesion to organic polymers, (1987).

14. Drzal, L. T., Sugiura, N., and Hook, D. Fiber-matrix chemical bonding in composite materials and its effect on adhesion. *Abstracts Of Papers Of The American Chemical Society* **212**, 4–POLY (1996).

15. Applied Research Lab (ARL) Penn State Composite Material Division Carbon Fiber Composite Fabrication, (2004).

16. Bunsell, A. R. and Renard, J. *Fundamentals of Fibre Reinforced Composite Materials*, volume 1 of *Series in Materials Science and Engineering*. Institute of Physics, Philadelphia, (2005).

17. Miller, T. E., editor. *Introduction to Composites*. SPI Composites Institute, 4th edition, (1997).

18. Jones, F. R. *Handbook of Polymer-Fibre Composites*. Polymer Science and Technology Series. John Wiley and Sons, New York, (1994).

19. Batch, G. L. and Macosko, C. W. Kinetic-model for cross-linking free-radical polymerization including diffusion limitations. *Journal Of Applied Polymer Science* **44**(10), 1711–1729 (1992).

20. Cook, W. D., Simon, G. P., Burchill, P. J., Lau, M., and Fitch, T. J. Curing kinetics and thermal properties of vinyl ester resins. *Journal Of Applied Polymer Science* **64**(4), 769–781 (1997).

21. Li, L., Sun, X. D., and Lee, L. J. Low temperature cure of vinyl ester resins. *Polymer Engineering And Science* **39**(4), 646–661 (1999).

22. Sorathia, U., Ness, J., and Blum, M. Fire safety of composites in the US Navy. *Composites Part A-Applied Science And Manufacturing* **30**(5), 707–713 (1999).

23. Fitzer, E. Pan-based carbon-fibers present state and trend of the technology from the viewpoint of possibilities and limits to influence and to control the fiber properties by the process parameters. *Carbon* **27**(5), 621–645 (1989).

24. McNaught, A. D. and Wilkinson, A. *Compendium of chemical terminology: IUPAC recommendations*, volume 2. Blackwell Science, (1997).

25. Cahn, R., Haasen, P., and Kramer, E., editors. *Materials Science and Technology: A Comprehensive Treatment*, volume 13 of *Structure and Properties of Composites*. Weinheim, New York, (1993).

26. Committee on High-Performance Structural Fibers for Advanced Polymer Matrix Composites, N. R. C. *High-Performance Structural Fibers for Advanced Polymer Matrix Composites*. The National Academies Press, Washington, D.C., (2005).

27. Toensmeier, P. A. Advanced composites soar to new heights in Boeing 787. *Plastics Engineering* **61**(8), 8 (2005).

28. Chung, D. D. L. *Carbon Fiber Composites*. Butterworth-Heinemann, Boston, (1994).

29. Donnet, J. *Carbon Fibers*. Marcel Dekker, New York, 3rd edition, (1998).

30. Berthelot, J. *Composite Materials: Mechanical Behavior and Structural Analysis*. Mechanical Engineering Series. Springer, New York, 1st edition, (1999).

31. Sharpe, L. Interphase in adhesion. *The Journal of Adhesion* **4**(1), 51 (1972).

32. Drzal, L. T., Rich, M. J., and Lloyd, P. F. Adhesion of graphite fibers to epoxy matrices - the role of fiber surface-treatment. *Journal Of Adhesion* **16**(1), 1–30 (1983).

33. Baley, C., Davies, P., Grohens, Y., and Dolto, G. Application of interlaminar tests to marine composites. *Applied Composite Materials* **11**(2), 99–126 (2004).

34. Herrerafranco, P. J. and Drzal, L. T. Comparison of methods for the measurement of fiber matrix adhesion in composites. *Composites* **23**(1), 2–27 (1992).

35. Moore, D. R. and Cervenka, A. Future requirements in the characterization of continuous fiber-reinforced polymeric composites (IUPAC technical report). *Pure And Applied Chemistry* **74**(4), 601–628 (2002).

36. Fitzer, E. and Weiss, R. Effect of surface-treatment and sizing of C-fibers on the mechanical properties of CFR thermosetting and thermoplastic polymers. *Carbon* **25**(4), 455–467 (1987).

37. Broyles, N. S., Verghese, K. N. E., Davis, R. M., Lesko, J. J., and Riffle, J. S. Pultruded carbon fiber vinyl ester composites processed with different fiber sizing agents: Processing and static mechanical performance. *Journal Of Materials In Civil Engineering* **17**(3), 320–333 (2005).

38. Kaverov, A., Kazakov, M., and Varshavsky, V. *Fibre Science and Technology*. Soviet advanced composites technology series. Chapman and Hall, London; New York, 1st edition, (1995).

39. Rich, M., Corbin, S., and Drzal, L. T. Adhesion of carbon fibers to vinyl ester matrices (SME technical paper AD00-241). In *Society of Manufacturing Engineers*, 10, (2000).

40. Gardner, S. D., He, G., and Pittman, C. U. A spectroscopic examination of carbon fiber cross sections using XPS and ISS. *Carbon* **34**(10), 1221–1228 (1996).

41. Ohwaki, T. and Ishida, H. Comparison between FT-IR and XPS characterization of carbon fiber surfaces. *Journal Of Adhesion* **52**(1-4), 167–186 (1995).

42. Ishitani, A. Application of X-ray photoelectron spectroscopy to surface analysis of carbon-fiber. *Carbon* **19**(4), 269–275 (1981).

43. Donnet, J. B. Chemical reactivity of carbons. *Carbon* **6**(2), 161 (1968).

44. Sellitti, C., Koenig, J. L., and Ishida, H. Surface characterization of graphitized carbon-fibers by attenuated total reflection fourier-transform infrared-spectroscopy. *Carbon* **28**(1), 221–228 (1990).

45. Denison, P., Jones, F. R., and Watts, J. F. The use of XPS and labeling techniques to study the surface-chemistry of carbon fibers. *Journal Of Physics D-Applied Physics* **20**(3), 306–310 (1987).

46. Mahy, J., Jenneskens, L. W., Grabandt, O., Venema, A., and Vanhouwelingen, G. D. B. The relation between carbon-fiber surface-treatment and the fiber surface microstructure. *Surface And Interface Analysis* **21**(1), 1–13 (1994).

47. Drzal, L. T., Madhukar, M., and Waterbury, M. C. Adhesion to carbon-fiber surfaces - surface chemical and energetic effects. *Composite Structures* **27**(1-2), 65–71 (1994).

48. Bradley, R. H., Ling, X., and Sutherland, I. An investigation of carbon-fiber surface-chemistry and reactivity based on XPS and surface free-energy. *Carbon* **31**(7), 1115–1120 (1993).

49. Ehrburger, P., Herque, J., and Donnet, J. B. Interface properties of carbon fibre composites. In *Fifth London International Carbon and Graphite Conference*, volume 1. Society of Chemical Industry, (1978).

50. Ryu, S. K., Park, B. J., and Park, S. J. XPS analysis of carbon fiber surfaces - anodized and interfacial effects in fiber-epoxy composites. *Journal Of Colloid And Interface Science* **215**(1), 167–169 (1999).

51. Park, S. J. and Kim, M. H. Effect of acidic anode treatment on carbon fibers for increasing fiber-matrix adhesion and its relationship to interlaminar shear strength of composites. *Journal Of Materials Science* **35**(8), 1901–1905 (2000).

52. Palmese, G. R., Andersen, O. A., and Karbhari, V. M. Effect of glass fiber sizing on the cure kinetics of vinyl-ester resins. *Composites Part A-Applied Science And Manufacturing* **30**(1), 11–18 (1999).

53. Ishida, H. and Koenig, J. L. Investigation of the coupling agent matrix interface of fiberglass reinforced-plastics by fourier-transform infrared spectroscopy. *Journal Of Polymer Science Part B-Polymer Physics* **17**(4), 615–626 (1979).

54. Lee, D. S. and Han, C. D. Effect of particulates and fiber reinforcements on the curing behavior of unsaturated polyester resin. *Journal Of Applied Polymer Science* **33**(2), 419–429 (1987).

55. Plueddemann, E. and Stark, G. L. Catalytic and electrokinetic effects in bonding through silanes. *Modern Plastics* **51**(3) (1974).

56. Tulig, T. J. and Tirrell, M. Toward a molecular theory of the trommsdorff effect. *Macromolecules* **14**(5), 1501–1511 (1981).

57. Drzal, L. T. and Madhukar, M. Fiber matrix adhesion and its relationship to composite mechanical-properties. *Journal Of Materials Science* **28**(3), 569–610 (1993).

58. Juska, T. and Puckett, P. Matrix resins and fiber/matrix adhesion. In Composites Engineering Handbook, Mallick, P. K., editor, 1249. New York (1997).

59. Stohr, J. *NEXAFS Spectroscopy*. Springer-Verlag, New York, (1992).

60. Stohr, J. and Jaeger, R. Absorption-edge resonances, core-hole screening, and orientation of chemisorbed molecules. *Physical Review B* **26**(8), 4111–4131 (1982).

61. Stohr, J. and Outka, D. A. Determination of molecular orientations on surfaces from the angular-dependence of near edge X-ray absorption fine structure spectra. *Physical Review B* **36**(15), 7891–7905 (1987).

62. Moad, G. and Solomon, D. H. *The Chemistry of Free Radical Polymerization*. Pergamon, New York, (1995).

63. Raghavendran, V. K., Drzal, L. T., and Askeland, P. Effect of surface oxygen content and roughness on interfacial adhesion in carbon fiber-polycarbonate composites. *Journal Of Adhesion Science And Technology* **16**(10), 1283–1306 (2002).

64. Scott, T. F., Cook, W. D., and Forsythe, J. S. Kinetics and network structure of thermally cured vinyl ester resins. *European Polymer Journal* **38**(4), 705–716 (2002).

65. Albertin, L., Stenzel, M. H., Barner-Kowollik, C., Foster, L. J. R., and Davis, T. P. Solvent and oxygen effects on the free radical polymerization of 6-O-vinyladipoyl-D-glucopyranose. *Polymer* **46**(9), 2831–2835 (2005).

66. Moulder, J. and Chastain, J. *Handbook of x-ray photoelectron spectroscopy*. Perkin-Elmer Corporatioon, Physical Electronics Division, (1992).

67. Oyama, H. T. and Wightman, J. P. Surface characterization of pvp-sized and oxygen plasma-treated carbon fibers. *Surface And Interface Analysis* **26**(1), 39–55 (1998).

68. Desimoni, E., Casella, G. I., Morone, A., and Salvi, A. M. XPS determination of oxygen-containing functional-groups on carbon-fiber surfaces and the cleaning of these surfaces. *Surface And Interface Analysis* **15**(10), 627–634 (1990).

69. Proctor, A. and Sherwood, P. M. A. X-ray photoelectron spectroscopic studies of carbon-fiber surfaces. 3. industrially treated fibers and the effect of heat and exposure to oxygen. *Surface And Interface Analysis* **4**(5), 212–219 (1982).

70. Xie, Y. M. and Sherwood, P. M. A. X-ray photoelectron spectroscopic studies of carbon-fiber surfaces. 11. differences in the surface-chemistry and bulk structure of different carbon-fibers based on poly(acrylonitrile) and pitch and comparison with various graphite samples. *Chemistry Of Materials* **2**(3), 293–299 (1990).

71. Kozlowski, C. and Sherwood, P. M. A. X-ray photoelectron-spectroscopic studies of carbon-fibre surfaces. 5. the effect of Ph on surface oxidation. *Journal Of The Chemical Society-Faraday Transactions I* **81**, 2745–2756 (1985).

72. Wang, Y. Q., Viswanathan, H., Audi, A. A., and Sherwood, P. M. A. X-ray photoelectron spectroscopic studies of carbon fiber surfaces. 22. comparison between surface treatment of untreated and previously surface-treated fibers. *Chemistry Of Materials* **12**(4), 1100–1107 (2000).

73. Proctor, A. and Sherwood, P. M. A. X-ray photo-electron spectroscopic studies of carbon-fiber surfaces. 1. carbon-fiber spectra and the effects of heat-treatment. *Journal Of Electron Spectroscopy And Related Phenomena* **27**(1), 39–56 (1982).

74. Desaeger, M., Reis, M. J., doRego, A. M. B., daSilva, J. D. L., and Verpoest, I. Surface characterization of poly(acrylonitrile) based intermediate modulus carbon fibres. *Journal Of Materials Science* **31**(23), 6305–6315 (1996).

75. Chiang, Y. C., Lee, C. Y., and Lee, H. C. Surface chemistry of polyacrylonitrile- and rayon-based activated carbon fibers after post-heat treatment. *Materials Chemistry And Physics* **101**(1), 199–210 (2007).

76. Buttry, D. A., Peng, J. C. M., Donnet, J. B., and Rebouillat, S. Immobilization of amines at carbon fiber surfaces. *Carbon* **37**(12), 1929–1940 (1999).

77. Weng, L. T., Poleunis, C., Bertrand, P., Carlier, V., Sclavons, M., Franquinet, P., and Legras, R. Sizing removal and functionalization of the carbon-fiber surface studied by combined SIMS and XPS. *Journal Of Adhesion Science And Technology* **9**(7), 859–871 (1995).

78. Braun, A., Huggins, F. E., Kelly, K. E., Mun, B. S., Ehrlich, S. N., and Huffman, G. P. Impact of ferrocene on the structure of diesel exhaust soot as probed with wide-angle X-ray scattering and C(1s) NEXAFS spectroscopy. *Carbon* **44**(14), 2904–2911 (2006).

79. Cody, G. D., Ade, H., Wirick, S., Mitchell, G. D., and Davis, A. Determination of chemical-structural changes in vitrinite accompanying luminescence alteration using C-NEXAFS analysis. *Organic Geochemistry* **28**(7-8), 441–455 (1998).

80. Francis, J. T. and Hitchcock, A. P. Inner-shell spectroscopy of para-benzoquinone, hydroquinone, and phenol - distinguishing quinoid and benzenoid structures. *Journal Of Physical Chemistry* **96**(16), 6598–6610 (1992).

81. Braun, A., Huggins, F. E., Shah, N., Chen, Y., Wirick, S., Mun, S. B., Jacobsen, C., and Huffman, G. P. Advantages of soft X-ray absorption over TEM-EELS for solid carbon studies - a comparative study on diesel soot with EELS and NEXAFS. *Carbon* **43**(1), 117–124 (2005).

82. Zhu, Q., Money, S. L., Russell, A. E., and Thomas, K. M. Determination of the fate of nitrogen functionality in carbonaceous materials during pyrolysis and combustion using X-ray absorption near edge structure spectroscopy. *Langmuir* **13**(7), 2149–2157 (1997).

83. Gago, R., Jimenez, I., Albella, J. M., and Terminello, L. J. Identification of ternary boron-carbon-nitrogen hexagonal phases by x-ray absorption spectroscopy. *Applied Physics Letters* **78**(22), 3430–3432 (2001).

84. Painter, P. C., Snyder, R. W., Starsinic, M., Coleman, M. M., Kuehn, D. W., and Davis, A. Concerning the application of FTIR to the study of coal - a critical-assessment of band assignments and the application of spectral-analysis programs. *Applied Spectroscopy* **35**(5), 475–485 (1981).

85. Painter, P. C., Starsinic, M., Squires, E., and Davis, A. A. Concerning the 1600 cm-1 region in the IR-spectrum of coal. *Fuel* **62**(6), 742–744 (1983).

86. Starsinic, M., Taylor, R. L., Walker, P. L., and Painter, P. C. FTIR studies of saran chars. *Carbon* **21**(1), 69–74 (1983).

87. Juska, T. VARTM of Composite Panels Fabricated with Vinyl Ester Resin and Oxidized Carbon Fiber Reinforcements, (c. 2005).